

A modelling platform for climate change impact on local and regional crop water requirements

Questa è la versione Post print del seguente articolo:

Original

A modelling platform for climate change impact on local and regional crop water requirements / Masia, S., Trabucco, A., Spano, D., Snyder, R.L., Susnik, J., Marras, S.. - In: AGRICULTURAL WATER MANAGEMENT. - ISSN 0378-3774. - 255:1(2021). [10.1016/j.agwat.2021.107005]

Availability:

This version is available at: 11388/247495 since: 2022-07-26T10:42:52Z

Publisher:

Published

DOI:10.1016/j.agwat.2021.107005

Terms of use:

Chiunque può accedere liberamente al full text dei lavori resi disponibili come "Open Access".

Publisher copyright

note finali coverpage

(Article begins on next page)

This is the Author's accepted manuscript version of the following contribution:

A modelling platform for climate change impact on local and regional crop water requirements

The publisher's version is available at: [10.1016/j.agwat.2021.107005](https://doi.org/10.1016/j.agwat.2021.107005)

When citing, please refer to the published version.

Manuscript Details

Manuscript number AGWAT_2020_1285

Title A Modeling Tool to Assess the Impact of Climate Change on Crop Water Requirement at Local and Regional Scale

Abstract

The impact of climate change on agriculture is projected to be more severe over the coming years due to changing intensity, magnitude and distribution of precipitation, soil water content, atmospheric water vapor, higher temperatures, and thus larger evapotranspiration. This will have significant consequences for irrigation requirements, especially in semi-arid area of Southern Europe recognized as hotspot of climate change. Since the total water use to satisfy agricultural demand is currently about 25% of total water withdrawal in Europe and up to 80% in some Mediterranean countries, improvements in water use management are needed to cope with worsening climate conditions. Although several crops and hydrological models have been developed, only a few couple crop growth, soil water flow, and irrigation mechanics to assess agricultural water management both at local and regional scale. In this work, the Simulation of Evapotranspiration of Applied Water (SIMETAW#) model is implemented in R with two new versions able to estimate crop water consumption, irrigation demand and scheduling at local (SIMETAW_R) and regional scale (SIMETAW_GIS platform) using extensive climate and environmental geospatial datasets. SIMETAW_R was validated in ten experimental sites, and SIMETAW_GIS performance in Mediterranean countries was assessed by estimating the impact of climate change on maize, wheat, and wine grape water needs in the past (1976-2005) and future climate conditions (2036-2065), under RCP4.5 and RCP8.5 scenarios. Results showed that in Mediterranean countries, maize, wheat, and grape production will require on average about 13%, 16%, and 10% more water, respectively, under future climate, representing a considerable challenge for water resources management, especially with demand increases in other sectors. The tool showed great potential in estimating climate change impact on crop water consumption and irrigation requirements, both at local and regional scale, and offers new analytical skills for water resources management planners for improved decision-making.

Submission Files Included in this PDF

File Name [File Type]

Masia et al._Highlights.docx [Highlights]

Masia et al._Manuscript.docx [Manuscript File]

Masia et al._Figures.docx [Figure]

Masia et al._Tables.docx [Table]

To view all the submission files, including those not included in the PDF, click on the manuscript title on your EVISE Homepage, then click 'Download zip file'.

A Modeling Tool to Assess the Impact of Climate Change on Crop Water Requirement at Local and Regional Scale

Highlights:

- New SIMETAW# versions (-R and -GIS) are introduced, described, and tested.
- Great potential in estimating climate change impact on crop water requirements.
- Maize, wheat, and grape irrigation demand is expected to rise under climate change.
- Increases in water-related issues in the Mediterranean basin are highlighted.
- Both tools could be used to address decision making at local and regional scale.

A Modeling Tool to Assess the Impact of Climate Change on Crop Water Requirement at Local and Regional Scale

Sara Masia^{1*}, Antonio Trabucco^{2,3}, Donatella Spano^{2,3}, Richard L. Snyder⁴, Janez Sušnik¹, Serena Marras^{2,3}

¹ Land and Water Management Department, IHE Delft Institute for Water Education, Westvest 7, 2611 AX Delft, The Netherlands

² Department of Agriculture, University of Sassari, Viale Italia, 39, 07100 Sassari, Italy

³ CMCC Foundation – Euro-Mediterranean Centre on Climate Change, IAFES Division, Viale Italia 39, 07100 Sassari, Italy

⁴ Land, Air and Water Resources Department, University of California, One Shields Ave., Davis, CA 95616, USA

*Corresponding author: s.masia@un-ihe.org

Highlights:

- New SIMETAW# versions (-R and -GIS) are introduced, described, and tested.
- Great potential in estimating climate change impact on crop water requirements.
- Maize, wheat, and grape irrigation demand is expected to rise under climate change.
- Increases in water-related issues in the Mediterranean basin are highlighted.
- Both tools could be used to address decision making at local and regional scale.

Abstract

The impact of climate change on agriculture is projected to be more severe over the coming years due to changing intensity, magnitude and distribution of precipitation, soil water content, atmospheric water vapor, higher temperatures, and thus larger evapotranspiration. This will have significant consequences for irrigation requirements, especially in semi-arid area of Southern Europe recognized as hotspot of climate change. Since the total water use to satisfy agricultural demand is currently about 25% of total water withdrawal in Europe and up to 80% in some Mediterranean countries, improvements in water use management are needed to cope with worsening climate conditions. Although several crops and hydrological models have been developed, only a few couple crop growth, soil water flow, and irrigation mechanics to assess agricultural water management both at local and regional scale. In this work, the Simulation of Evapotranspiration of Applied Water (SIMETAW#) model is implemented in R with two new versions able to estimate crop water consumption, irrigation demand and scheduling at local (SIMETAW_R) and regional scale (SIMETAW_GIS platform) using extensive climate and environmental geospatial datasets. SIMETAW_R was validated in ten experimental sites, and SIMETAW_GIS performance in Mediterranean countries was assessed by estimating the impact of climate change on maize, wheat, and wine grape water needs in the past (1976-2005) and future climate conditions (2036-2065), under RCP4.5 and RCP8.5 scenarios. Results showed that in Mediterranean countries, maize, wheat, and grape production will require on average about 13%, 16%, and 10% more water, respectively, under future climate, representing a considerable challenge for water resources management, especially with demand increases in other sectors. The tool showed great potential in estimating climate change impact on crop water consumption and irrigation requirements, both at local and regional scale, and offers new analytical skills for water resources management planners for improved decision-making.

47

48 **Keywords:**

49 SIMETA model, spatial modeling, water scarcity, RCPs, crop irrigation requirement,
50 evapotranspiration.

51

52 **1. Introduction**

53 Climate change is one of the most important challenges in the 21st century. The
54 Intergovernmental Panel on Climate Change (IPCC) stated that climate-related hazards will
55 worsen in the coming decades with significant variations in the Earth's climate (IPCC, 2013;
56 IPCC 2018a). Rising greenhouse gas (GHG) concentration in the atmosphere is causing strong
57 changes in the hydrological cycle (IPCC, 2014; Kleidon and Renner, 2018) that are expected
58 to intensify by the end of the century when high flood frequency and perennial drought may
59 characterize large areas (IPCC, 2018b; EEA 2019).

60 Climate models foresee non-uniform variation in global hydrological cycles. An increase of
61 annual precipitation in Northern Europe and a strong reduction in the number of rainy days
62 with a consequent higher risk of drought periods is predicted in central Europe and
63 Mediterranean areas (IPCC, 2013). Water scarcity is expected to increase worldwide, and this
64 trend will be exacerbated not only by climate change but also by demographic growth, socio-
65 economic development, increasing demand for raw materials and energy, extension of
66 residential centres, as well as improvement of quality of life and technology (Brooks, 2012).
67 Increasing competition for water resources, threatening a sustainable balance between water
68 demand and supply, is expected to worsen water scarcity globally, with the Mediterranean
69 expected to be a water scarcity 'hotspot' (Giorgi 2006; OECD, 2017; Cramer 2018).

70 Agriculture is one of the most water demanding sectors in Mediterranean countries. The
71 agricultural sector is responsible for about 70% of water withdrawal globally (World Bank,
72 2017), while is about 25% at European level, where the percentage in Central and Western
73 parts (27%) is slightly higher than in Eastern areas (21%) (FAO, 2016). This is much higher in
74 southern Europe and Mediterranean area, where some countries stand out with extremely high
75 values, i.e., Syria (88%), Morocco (87%), Egypt (86%), and Libya (83%) (Climate-ADAPT,
76 2016; Ferragina and Canitano, 2014). In some Southern and Eastern Mediterranean countries,
77 Ferragina and Canitano (2014) reported that the Water Exploitation Index (WEI, where WEI >
78 40% indicates a water stress conditions) is far higher than 40% (99% in Jordan, 94% in Egypt,
79 86% in Syria, and 80% in Israel), highlighting a severe impact on renewable water resource
80 exploitation, and suggesting a significant water management challenge under changing water
81 and socio-economic conditions. The overexploitation of both surface and ground water
82 resources requires further efforts to improve irrigation efficiency to compensate increases in
83 crop water demand due to climate change, and to identify strategies to sustain food security
84 (Fader et al., 2016; Masia et al., 2018).

85 Despite the high percentages of agricultural water use, it is crucial to emphasize the water-food
86 nexus to explain the critical role of water to guarantee food security to supply the growing
87 population, to alleviate poverty, and to stimulate the rural socio-economic development
88 (Ferragina and Canitano, 2014; World Bank, 2017). Given the large irrigated areas in the
89 Mediterranean regions and projected influence of climate change, the development of models
90 in the agricultural sector becomes essential to simulate current and expected future water
91 requirements under different emissions scenarios, climatic conditions and crop management
92 regimes. This can help farmers, decision and policy makers to develop optimal strategies
93 balancing economic growth and environmental sustainability (i.e. water demand vs available
94 resources).

95 Although the number of crop models (e.g. WOFOST, van Diepen et al., 1989; EPIC,
 96 Williams, 1990; CROPSYST; Stockle et al., 2003; CERES-Maize, Bao et al., 2017) and
 97 hydrological models (SWAT, Santhi et al., 2001; DREAM, Monfreda et al., 2005; Wasim-
 98 ETH, Schulla and Jasper, 2007), is rising, more effort is needed to improve the simulation on
 99 the effect of irrigation management and practices, together with soil water balance and crop
 100 water consumption, with outcomes on irrigation demand, crop growth and yield, both at local
 101 and regional scale. Even though model coupling is still at an early stage (Siad et al., 2019),
 102 there is an advantage of this approach for quantifying interactions among different elements in
 103 complex systems. More specifically, there is a growing need of coupled models that are able
 104 to estimate and forecast atmosphere-soil-water-crop-irrigation applications interactions at
 105 different time and spatial scale in order to improve water system management.

106 In this work, the Simulation of Evapotranspiration of Applied Water model (SIMETAW#
 107 model; Mancosu et al., 2016), which is able to estimate the daily reference crop and actual
 108 evapotranspiration (ET_o , ET_c , ET_a), the evapotranspiration of applied water (ET_{aw}), irrigation
 109 scheduling, and the rainfed and irrigated crop growth and yield for a specific experimental site,
 110 was implemented in the R platform (SIMETAW_R) to estimate crop consumption and
 111 irrigation requirements at local scale. The new tool was integrated into a GIS spatial platform
 112 under R, thus named SIMETAW_GIS, which couples and processes different geospatial
 113 climate and environmental data and reiterates simulations over regional scales. The aim of this
 114 paper is to introduce and demonstrate both new SIMETAW# versions (-R and -GIS), and
 115 highlight their added value for water resources planning and management under expected
 116 climate change conditions.

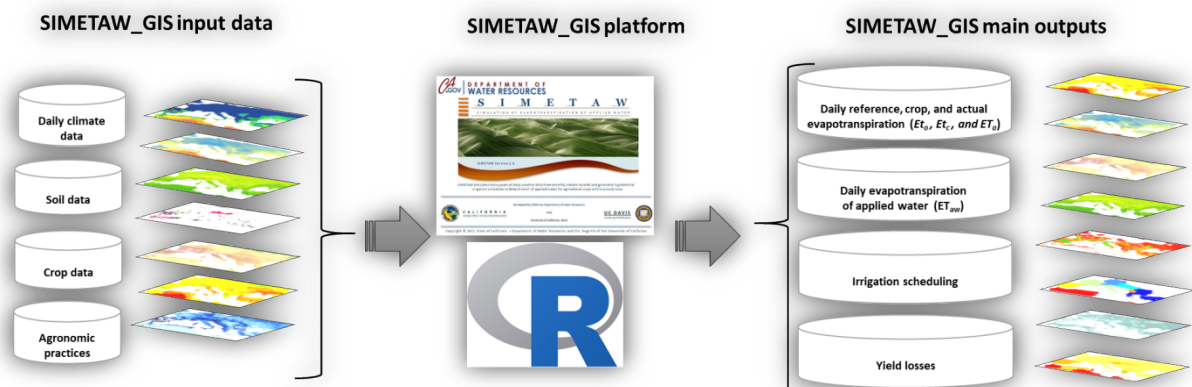
117

118 2. Materials and Methods

119

120 2.1 SIMETAW_R and SIMETAW_GIS model description

121 Two new versions of SIMETAW#, (Mancosu et al., 2016) are introduced, described, and tested
 122 in this work. The new versions are able to perform at local (i.e. site specific) “SIMETAW_R”
 123 and wider spatial scale “SIMETAW_GIS” (Figure 1). Full details of the original SIMETAW#
 124 model is found in Mancosu et al. (2016).



125


126

127

128 *Fig. 1. Scheme of SIMETAW_GIS platform.*

129 The SIMETAW_R modelling scheme, designed for site-specific applications, was
 130 validated at 10 experimental sites, and then implemented for spatially distributed applications
 131 using GIS libraries available in R within the spatial platform named SIMETAW_GIS (Figure
 132 1). The spatial platform couples and automates interactions with large geodatasets of climate
 133 variables, environmental conditions, and agronomic practices, to process the soil water balance
 for multiple years and pixels across regional and continental scales. SIMETAW_GIS was


134 tested by running regional simulation of water consumption and net water application in the
135 **Mediterranean domain** (www.cordex.org) under past (1976-2005) and future (2036-2065)
136 climate conditions, under RCP 4.5 and RCP 8.5 scenarios. Both versions were tested for grape,
137 maize, and wheat.

138 SIMETAW#/R/GIS are daily crop-soil-water balance grams developed to compute
139 the reference evapotranspiration (ET_o), the crop evapotranspiration (ET_c), the actual
140 evapotranspiration (ET_a), and the evapotranspiration of applied water (ET_{aw}). Note that ET_o is
141 the evapotranspiration from a virtual reference surface having known aerodynamic and canopy
142 resistances and is based on an equation using data from a well-designed and managed weather
143 station surrounded by an extensive grass surface. While the surface is virtual, the equation was
144 developed by comparing it with energy-limited evapotranspiration from a well-watered 12 cm
145 tall, cool-season grass. The crop evapotranspiration (ET_c) is the energy limited
146 evapotranspiration from a large field of a well-watered, healthy crop that is experiencing little
147 or no stress. The ET_a is actual evapotranspiration, which is what would be measured over a
148 crop whether stressed or not. The energy limited ET_c is calculated as: $ET_c = ET_o \times K_c$ where K_c
149 is the crop coefficient. The actual ET_a is calculated as: $ET_a = ET_c \times K_s$ where K_s is the stress
150 coefficient. Note that $K_s = 0.00$ when there is no ET and $K_s = 1.00$ when there is no ET reducing
151 stress and $ET_a = ET_c$. In addition, the actual ET_a is calculated as: $ET_a = ET_o \times K_c \times K_s = ET_o \times K_a$
152 where K_a is the actual coefficient.

153 The ET of applied water (ET_{aw}) is an estimate of how much water from the irrigation
154 of a crop contributes to the crop evapotranspiration during a season. It does not include water
155 from other sources like pre-season stored soil water, in-season effective rainfall, seepage from
156 levees or water from water tables. Once the ET_{aw} is estimated, the required water diversion for
157 irrigation can be assessed by dividing the ET_{aw} by the irrigation system Distribution Uniformity
158 (DU) assuming that the low quarter¹ is refilled at each irrigation.

159 The ET_{aw} is calculated as:

$$160$$
$$161 \quad ET_{aw} = \sum_{i=1}^n NA_i = CET_c - CE_{spg} - CE_r - \Delta SW \quad (1)$$
$$162$$

163 **where** $\sum_{i=1}^n NA_i$ is the sum of the net applications (i.e., depths applied to the low quarter of the
164 field), CET_c is the cumulative ET_c , CE_{spg} is the cumulative seepage or water table contribution,
165 and CE_r is the cumulative effective rainfall during the season .

166 SIMETAW estimates the amount of water required by irrigated crops, schedules the
167 number of irrigation events, and the net amount of water to be applied per each event (net
168 application; NA). The "SIMETAW#" model was improved by integrating into SIMETAW_R
169 and GIS program the computation of the reference evapotranspiration (ET_o). Daily ET_o is
170 estimated with three alternative methods: (i) the original equation from Hargreaves and
171 Samani-HS (1985); (ii) the modified HS equation (Samani, 2000) (ET_{o_HS}), and standardized

¹ The low quarter water application is the mean irrigation applied to the quarter which receives the least amount of water, while the high quarter water application is the mean depth of water applied to the quarter which receives the largest quantity of water. The second and the third quarters water application are the mean depths of water applied to the intermediate quarters (Mancosu et al, 2016).

172 reference evapotranspiration equation for short canopies (ET_o_{PM}) (Allen et al., 1998; Allen
 173 et al., 2005; Allen et al., 2006). Following Snyder (2012), the model adjusts the canopy
 174 resistance (r_c , eq. 2) allowing the assessment of the effect of CO_2 concentration changes in the
 175 atmosphere.

$$176 \quad r_c = \frac{1000}{1.44(14.18 - 0.0112CO_2)} \quad (\text{m s}^{-1}) \quad (2)$$

178
 179 One of the most relevant characteristics of the model is that it computes the seasonal crop
 180 coefficient (K_c) trend using inflection points identified as a percentage of the growing season
 181 and daily K_c values at the beginning of the season, midseason, and at the end of late season to
 182 define the seasonal crop coefficient changes. This allows users to easily define the daily crop
 183 coefficients they need by changing the starting and ending of the growing season dates.

184 SIMETAW allows for adjustment of the midseason K_c (K_{Cmid}) as a function of the local
 185 climate as:

$$186 \quad K_{Cmid} = K_{ctab} + 0.261 \cdot (ET_0 - 7.3) \cdot (K_{ctab} - 1) \quad (3)$$

188
 189 where K_{ctab} is the tabular K_c from research that is expected in a climate with $ET_o \approx 7.3$ mm day⁻¹
 190 (Guerra et al., 2014). Crops with a $K_{Cmid} > 1.00$ in areas with ET_o of 7.3 mm day⁻¹ will have a
 191 higher K_{Cmid} in a climate with $ET_o > 7.3$. In a climate with $ET_o < 7.3$ mm day⁻¹, a lower K_{Cmid} is
 192 expected.

193 The allowable depletion (AD), i.e. the amount of available water which corresponds to
 194 the yield threshold depletion, is a default value in the model equal to 50% of the plant available
 195 water. The model also estimates the soil water depletion ($SWD = FC - SWC$), where FC is the
 196 soil field capacity and SWC is the measured or estimated soil water content. The current day's
 197 SWD is calculated adding the SWD of the previous day (SWD_{i-1}), the crop evapotranspiration
 198 of the current day (ET_{ci}), the capillary rise from a water table or seepage (C_i), percolation below
 199 the root layer (D_i), the depth of irrigation (I_i), and the runoff (R_{offi}) (eq. 4). When precipitation
 200 (P_{cpi}) is higher than SWD , then the effective rainfall is $R_e = SWD$, otherwise $R_e = P_{cpi}$ (Mancosu
 201 et al., 2016). In the first case, the SWC returns to field capacity and (FC) is achieved, while in
 202 the second case the $SWC < FC$.

$$203 \quad SWD_i = SWD_{i-1} + ET_{ci} + P_{cpi} + C_i - D_i - R_{offi} + I_i \quad (\text{mm}) \quad (4)$$

205
 206 The calculation of daily soil water depletion is necessary to define the irrigation events that
 207 occur before the SWD exceeds the management of allowable depletion (MAD, mm), thus the
 208 computation of MAD is essential to define irrigation scheduling.

209 MAD is the amount of water that can be depleted between water irrigation applications
 210 without incurring water deficit. It is considered as the water amount necessary to refill the soil
 211 to field capacity (Net Application, NA, mm). The model computes the evapotranspiration of
 212 the applied water (ET_{aw} , mm), i.e. the sum of the net irrigation application ($\sum NA$).

213 At the end of the initial growth period, only 10% of soil is covered by the crop, in this
 214 growth stage the crop evaporation is considered equal to the soil evaporation process, thus NA
 215 is computed as:

$$216 \quad NA_c = \overline{ET}_0 \cdot K_e \cdot d_e \quad (\text{mm}) \quad (5)$$

218

219 where K_e is the coefficient of evaporation of bare soil, \overline{ET}_o (mm) represents the mean daily
 220 reference evapotranspiration during initial growth period (i.e. from planting to 10% ground
 221 shading), which is stage A to B of the growing season, and d_e the number of water applications
 222 during this time step. It is assumed that the ET from a crop having less than 10% ground
 223 shading is equal to bare soil evaporation. The K_e is computed as:

$$224 \quad K_e = \frac{2.54}{\sqrt{CET_o}} \quad (6)$$

226 where 2.54 represents a typical soil hydraulic factor and CET_o is the cumulative ET_o .

227 At the beginning of the mid-season NA_c is computed as:

$$228 \quad NA_c = (1 - R_{off}) \cdot RT \cdot AR \cdot D_u \quad (\text{mm}) \quad (7)$$

232 where RT is the runtime that depends on the irrigation method, AR is the application rate (mm
 233 h^{-1}), and D_u is the distribution uniformity expressed as a fraction (Mancosu et al., 2016). The
 234 program helps to plan for the number and frequency of irrigation events during the midseason
 235 in the case of full (100% water allocation percentage, $WAP = 100\%$) or deficit irrigation (WAP
 236 $< 100\%$). For fully irrigated crops, the number of water applications (N_{ic}) is computed as the
 237 ratio between the ET_{awe} and the management allowable depletion (MAD_c) in well-watered
 238 conditions:

$$239 \quad N_{ic} = \frac{ET_{awe}}{MAD_c} \quad (\text{mm}) \quad (8)$$

241 The number of water applications for deficit irrigation (N_{ia}) is computed assuming that the
 242 plant irrigation requirement (PIR) is less than 100%:

$$243 \quad N_{ia} = \frac{\sum NA_a}{MAD_c} \quad (\text{mm}) \quad (9)$$

244 where the sum of the irrigation depths applied to the low quarter of a crop cultivated in deficit
 245 irrigation conditions ($\sum NA_a$) is:

$$246 \quad \sum NA_a = (WA - \sum R_o) \cdot D_u \quad (\text{mm}) \quad (10)$$

249 where WA is the water allocation, i.e. the mean amount of water available for irrigation, R_o is
 250 the runoff coefficient and D_u the distribution uniformity. For a crop with water deficit, the
 251 actual MAD (MAD_a) is:

$$252 \quad MAD_a = \frac{\sum NA_a}{N_{ia}} \quad (\text{mm}) \quad (11)$$

255 The evapotranspiration of the applied water of a well-watered crop (ET_{awe}) is then computed as:

$$256 \quad ET_{awe} = CET_c - \left(YTD_c - \frac{YTD_{os}}{2} \right) \quad (\text{mm}) \quad (12)$$

259 where CET_c is the cumulate value of ET_c during the entire growing season, YTD_c is the yield
 260 threshold depletion during the mid-season, and YTD_{os} represents the yield threshold depletion
 261 during the off-season.

262
 263
 264
 265
 266
 267
 268
 269
 270
 271
 272
 273
 274
 275
 276
 277
 278
 279
 280
 281
 282
 283
 284
 285
 286
 287
 288
 289
 290
 291
 292
 293
 294
 295
 296
 297
 298
 299
 300
 301
 302
 303
 304
 305
 306
 307
 308

SIMETA_W# and SIMETA_W_R estimate the yield losses at a specific site considering that the irrigation in the field is not uniform (see Mancosu et al., 2016) while in SIMETA_W_GIS the yield losses at regional scale is computed following Steduto et al. (2009):

$$1 - \frac{Y_a}{Y_m} = K_y \cdot \left(1 - \frac{ET_a}{ET_c}\right) \quad (13)$$

where Y_a is the actual crop yield, Y_m the maximum expected crop yield, and K_y the yield response factor. This equation explains the link between water use and crop yield and shows how yield losses correspond to a reduction in evapotranspiration. Further details of the original SIMETA_W# model, are found in Mancosu et al. (2016).

2.2 SIMETA_W_R validation and SIMETA_W_GIS application.

2.2.1 SIMETA_W_R validation

SIMETA_W_R was validated at ten European sites (Table 1) selected through the international FLUXNET network (<http://fluxnet.fluxdata.org/>). Model performance was assessed by comparing actual evapotranspiration simulated by the model and the latent heat flux (LE) measured through the Eddy covariance technique in each site. LE was converted from $W\ m^{-2}$ to $MJ\ m^{-2}\ d^{-1}$ using the conversion factor of 0.0864 and from $MJ\ m^{-2}\ d^{-1}$ to $mm\ d^{-1}$ using the conversion factor of 0.408. Maize, wheat, and grape crop water consumption were estimated for each stage of the growing season and under different soil and climatic characteristics. Eddy covariance fluxes and climate data for each site were provided by meteorological, radiometric, and micrometeorological stations set up at each experimental site. In addition, a questionnaire was circulated to collect information about crop and soil characteristics and irrigation practices. Additional supplementary information was obtained through a literature review.

Pearson's coefficient (r), Root Mean Square Error (RMSE), Mean Bias error (MBE), Mean Absolute Error (MBA), and Index of Agreement (AI) were used to evaluate the SIMETA_W_R performance. In addition, model performance was explained by taking into account the percentage of gap filled observed data. Missing measured data were gap-filled following Falge et al. (2001). Days with less than 30% missing half-hourly observations were acceptable for the model evaluation.

The flux energy budget closure (EBC) was used to assess half-hour measured data reliability, by plotting the ratio $H+LE$ Vs R_n-G , where R_n is the net radiation ($W\ m^{-2}$), G is the soil heat flux ($W\ m^{-2}$), H is the sensible heat flux ($W\ m^{-2}$), and LE is the latent heat flux ($W\ m^{-2}$). Measured data are considered reliable when the sum of $H+LE$ is equal to R_n-G . According to the literature (Baldocchi et al., 1988; Twine et al., 2000; Wilson et al., 2002) an energy balance closure deviation of 20-30% is acceptable. The residual of the energy balance was also computed as $LE' = R_n - G - H$ to assess the quality of the half-hour measured data.

In addition, SIMETA_W_R performance in assessing ET_o was evaluated for both Hargreaves Samani (ET_o_{HS}) and the standardized FAO-56 Penman-Monteith (ET_o_{PM}) equations, calculated using gridded datasets and observed daily climate data obtained for each site. The E-OBS (European high-resolution gridded data set) gridded observation climate data (Haylock et al., 2008) and the COSMO-CLM RCM (Consortium for Small scale Modeling in Climate Model) (Rockel et al, 2008) forced by Era-Interim reanalysis were used as climate gridded datasets for the comparison.

Tab.1. *Crop characteristics and experimental sites selected through the FLUXNET network.*

Code	SITE	Country	Lat	Lon	Elevation (m.a.s.l.)	Crop	Sowing-Harvest date
------	------	---------	-----	-----	-------------------------	------	---------------------

IT-Neg	Negrisia	Italy	45.75	12.45	11	Wine Grape	01.04.2007/15.10.2007
IT-Neg	Negrisia	Italy	45.75	12.45	11	Wine Grape	01.04.2008/27.10.2008
IT-VdA	Valle dell'Adige	Italy	46.20	11.11	207	Wine Grape	15.04.2009/05.09.2009
IT-BCi	Borgo Cioffi	Italy	40.52	14.96	13	Maize	17.05.2005/24.08.2005
IT-BCi	Borgo Cioffi	Italy	40.52	14.96	13	Maize	27.04.2006/22.08.2006
IT-BCi	Borgo Cioffi	Italy	40.52	14.96	13	Maize	09.05.2007/24.08.2007
IT-BCi	Borgo Cioffi	Italy	40.52	14.96	13	Maize	12.06.2009/08.09.2009
DE-Kli	Klingenberg	Germany	50.89	13.52	468	Wheat	25.09.2005/06.09.2006
DE-Kli	Klingenberg	Germany	50.89	13.52	469	Maize	23.04.2007/2.10.2007
DE-Geb	Gebesee	Germany	51.10	10.91	157	Wheat	09.11.2006/07.08.2007
FR-Lam	Lamasquere	France	43.50	1.24	182	Wheat	18.10.2006/15.07.2007
FR-Lam	Lamasquere	France	43.50	1.24	182	maize	01.05.2006/31.08.2006
FR-Gri	Grignon	France	48.84	1.95	117	wheat	28.10.2005/15.07.2006
FR-Gri	Grignon	France	48.84	1.95	117	maize	09.5.2005/28.09.2005
CH-Oe2	Oensingen	Switzerland	47.29	7.73	450	wheat	19.10.2006/16.07.2007
BE-Lon	Lonzee	Belgium	50.55	4.75	165	wheat	14.10.2004/03.8.2005
BE-Lon	Lonzee	Belgium	50.55	4.75	165	wheat	13.10.2006/05.08.2007
NL-Dij	Dijgraaf	The Netherlands	51.99	5.65	9	maize	08.05.2007/27.09.2007

309

310 2.2.2 Climate data

311 The simulations covered the Mediterranean domain. Daily climate variables, over this domain,
 312 derived from the Global Circulation Model CMCC-MED (Coupled Model of Atmosphere-
 313 Ocean-Sea-Ice with a focus on Mediterranean region) developed by the Euro-Mediterranean
 314 Center on Climate Change (Scoccimarro et al., 2011; Gualdi et al., 2013) and downscaled to a
 315 spatial resolution of 14 km with the Regional Climate Model COSMO-CLM RCM, were used
 316 to estimate daily ET_c , ET_a , and ET_{aw} at Mediterranean scale for the baseline (1976-2005) and
 317 the future (2036-2065) climate periods.

318 The climate Representative Concentration Pathway (RCP) 4.5 and 8.5 scenarios, with
 319 projected radiative forcing for the future (Taylor et al., 2012) were used for climate change
 320 projections. The COSMO-CLM RCM forced by Era-Interim reanalysis (EI) produced by
 321 ECMWF (The European Centre for Medium-Range Weather Forecasts) (Dee et al., 2011) and
 322 the E-OBS data were used for assessing ET_o in the past period. EI data downscaled with
 323 COSMO-CLM RCM and E-OBS have a resolution of 14 and 21 km, respectively. E-OBS data
 324 are the result of the gridded interpolation of several meteorological stations over Europe. This
 325 dataset is known as the largest resolution of daily historical climate gridded dataset for Europe
 326 (Hofstra et al., 2009).

327

328 2.2.3 Soil and crop input data

329 Soil data were included in the soil water budget to compute ET_c , ET_a and ET_{aw} . The soil water
 330 holding capacity from the ISRIC-WISE (Global Data Set of Derived Soil Properties, 5 minutes
 331 Grid) (Batjes, 2000) database, and the maximum soil depth from the HWSO v1.2 (30 arc-
 332 second raster Harmonized World Soil Database) (Wieder et al., 2014) were used.
 333 The sowing and harvest date for maize and wheat, both under irrigated and rainfed conditions,
 334 were obtained from the AgMiP (Agricultural Model Inter-comparison and Improvement
 335 Project) database (Elliott et al., 2015).

336 A NetCDF file containing the mean grape bud break and harvest Julian Day (JD) was
 337 created. Mean values for the growing season stages were obtained from the literature and
 338 through the PEP725 database (Templ et al., 2018) (see Appendix 1). Three assumptions were
 339 made: i) the mean values are uniform within any country, ii) no differences in *Vitis vinifera*
 340 varieties between countries, and iii) the dates are averages of those found in the literature
 341 review (see Appendix 1). The countries included in the new gridded layer were selected
 342 considering a grape production area greater than 10,000 hectares according to FAOSTAT
 343 (<http://www.fao.org/faostat/en/#data/QC>) data, and the availability of bud break and harvest
 344 data from literature and from PEP725 database (Appendix 1).

345 The maximum rooting depths suggested by the FAO irrigation and drainage paper 56
346 (Allen et al., 1998) are used for crop at maturity and scaled down for the other stages.
347 Specifically, the maximum rooting depths of 50 mm (maize), 1650 mm (winter wheat), and
348 1500 mm (wine grape) were used.

349 The SPAM database (Spatial Production Allocation Model) from You et al. (2014), was
350 used to define the crop spatial distribution. The spatial crop allocation was expressed in
351 hectares both for irrigated and rainfed crops with a resolution of 5 minutes. Grape distribution
352 was obtained from the MIRCA 2000 (Global data set of monthly irrigated and rainfed crop
353 areas around the year 2000) database (Portmann et al., 2010).

354 2.2.3 Crop management data

356 The crops under investigation were not pre-irrigated. The reduction of planted land was not
357 taken into account, and the water application percentage, i.e. the percentage of full water
358 application for the specific crop allocated for the crop growing season (WAP), was set equal
359 to 100% for irrigated crops. The allowable depletion (AD) was set equal to 50% thus the yield
360 threshold depletion (YTD), when irrigation was applied, was equal to half of the plant available
361 water (PAW). The sprinkler irrigation method with a distribution uniformity (DU) of 75%, and
362 an application rate (AR) of 3.2 mm h⁻¹ was applied to run simulations for maize and irrigated
363 wheat at Mediterranean scale. The drip method was chosen to simulate grape water
364 consumption and the related net water applications. In this case, DU and AR were set equal to
365 85% and 0.7 mm h⁻¹, respectively. The runoff was set equal to zero. The use of neither
366 pesticides nor fertilisers is considered. The growing season is assumed not to change in future.

367 3. Results

369 Model performances are shown both at local and regional scale. Local simulations of ET_a are
370 compared with observed LE (converted to ET_a) (section 3.1.1), while at regional scale,
371 observed ET_a calculations are compared using gridded input data simulated by
372 SIMETAW_GIS (session 3.1.2). Model validation is accomplished by estimating ET_a in the
373 Mediterranean domain (section 3.2).

374 3.1 SIMETAW and GIS model validation

375 3.1.1. Evaluation of SIMETAW_R model performance in estimating actual 376 evapotranspiration at local scale

379 The SIMETAW_R performance are showed in Table 2. In general, the model performance was
380 good at all experimental sites. The promising ability of the model to estimate crop water
381 consumption is confirmed by the mean $r=0.80$, which was statistically significant at each site
382 ($P \leq 0.001$). Furthermore, the mean RMSE= 0.99 mm, mean MBE of 0.36 mm, mean MBA of
383 0.77 mm, and mean AI of 81% demonstrate high modelling performance for estimating ET_a
384 (Table 2).

385 In general, the model tends to slightly overestimate ET_a . The lowest and highest model
386 overestimation of ET_a were observed for wine grape, in IT-VdA (MBE = 0.06 mm) and IT-
387 Neg (MBE = 1.30 mm), respectively. The ET_a overestimation tendency was also reported in
388 Mancosu et al. (2016), where fruit tree evapotranspiration was assessed. The model
389 underestimates the actual crop water consumption in CH-Oe2, FR-Lam 2006-2007, and NL-
390 Dij sites during the rainfed season. However, best model performances are reported for the CH-
391 Oe2 site, where no LE data were gap filled. Even if only years with less than 30% of missing
392 half-hourly LE measured data, the amount of available meteorological and LE data affected
393 model performance. RMSE was, higher than 1.20 during each season in IT-Bci site, mainly

394 due to both a short period with a high percentage of LE gap-filled data and energy balance
 395 closure (Table 2). In general, the highest RMSE values have also a lower energy balance
 396 closure (Table 2). Some differences between measured and modelled data were attributed to
 397 rainy conditions during LE measurements that can reduce sensor accuracy when in measuring
 398 LE fluxes (Burba, 2013) even after quality check controls are performed.

399 In this work, the energy balance closure from available half-hour data (% of missing
 400 data is shown in Table 2) was acceptable with the mean slope of 0.75 and with the mean
 401 $R^2=81\%$ showing a good reliability of the Eddy covariance measured data. In addition, the
 402 measured data accuracy is shown by the mean $r=0.84$ between LE and LE' . The statistics in
 403 Table 2 indicate that the SIMETA_W_R model fits the observed data reasonably well, and could
 404 be used for predictive analysis for agricultural water management purposes.

405
 406 *Tab. 2. SIMETA_W_R performance shown through the comparison of observed and modelled ET_a in ten*
 407 *experimental sites. Measured data quality are shown through statistical indices, the energy balance*
 408 *closure (EBC) and the correlation between LE measured and LE residual (LE vs LE').*

Code	YEAR	Crop	Observed ET_a vs Modelled ET_a				EBC			LE vs LE'	
			r	RMSE mm	IA %	MBE mm	R^2 %	Y = aX + b	Gaps %	r	
FR-Gri	2005	Corn	0.81	0.75	89	0.04	0.63	91	Y = 0.7583X	19	0.89
FR-Gri	2005-2006	Wheat	0.85	0.61	91	0.12	0.45	87	Y = 0.6748X	16	0.87
DE-Geb	2006-2007	Wheat	0.75	1.14	78	0.69	0.78	77	Y = 0.7335X	15	0.85
DE-Kli	2007	Corn	0.84	1.39	67	1.23	1.24	56	Y = 0.4694X	32	0.61
DE-Kli	2005-2006	Wheat	0.88	0.82	88	0.57	0.65	67	Y = 0.8379X	33	0.62
CH-Oe2	2006-2007	Wheat	0.92	0.75	94	-0.44	0.58	68	Y = 0.8037X	34	0.82
NL-Dij	2007	Corn	0.71	0.68	82	-0.14	0.54	73	Y = 0.7905X	15	0.87
FR-Lam	2006-2007	Wheat	0.82	0.72	90	-0.23	0.55	83	Y = 0.7254X	41	0.83
FR-Lam	2006	Corn	0.61	1.22	76	0.43	0.92	90	Y = 0.7838X	42	0.91
BE-Lon	2006-2007	Wheat	0.78	0.91	82	0.57	0.72	82	Y = 0.8487X	20	0.84
BE-Lon	2004-2005	Wheat	0.89	0.89	90	0.14	0.65	82	Y = 0.8454X	23	0.85
IT-Bci	2005	Corn	0.64	1.21	73	0.62	0.92	92	Y = 0.7794X	26	0.92
IT-Bci	2006	Corn	0.62	1.29	69	0.73	0.97	86	Y = 0.7894X	39	0.82
IT-Bci	2007	Corn	0.63	1.48	68	0.93	1.12	94	Y = 0.778X	37	0.95
IT-Bci	2009	Corn	0.63	1.32	75	0.51	1.03	91	Y = 0.7405X	50	0.94
IT-VdA	2009	Wine Grape	0.82	0.68	90	0.06	0.5	77	Y = 0.6866X	23	0.93
IT-Neg	2007	Wine Grape	0.83	1.91	77	1.3	1.6	na*	na*	na*	na*
IT-Neg	2008	Wine Grape	0.58	2.45	67	1.31	1.88	na*	na*	na*	na*

* Soil heat flux (G) input data not available.

409
 410

3.1.2 SIMETA_W_GIS model performance in estimating reference evapotranspiration at regional scale

411
 412 The model computes ET_o using Hargreaves Samani equation (Hargreaves and Samani, 1985)
 413 and the standardized FAO-56 Penman-Monteith equation (Allen et al. 2005), by using the Era
 414 Interim (EI) and EOBS climate datasets to represent historical trends. The Penman Monteith
 415 (PM) method generally performs better than Hargreaves Samani (HS) equation for computing
 416 ET_o (Table 3). Unlike EI, the EOBS provides fewer climate variables sufficient to parameterize
 417 the HS method alone. Both HS and PM method can be implemented with EI. Correlation values
 418
 419

420 higher than 0.80 were computed by comparing gridded PM estimated ET_o using EI data with
 421 observations in almost all sites located in Northern Europe. The best correlations for HS and
 422 PM were obtained for crops with longer growing seasons as these data sets tend to have more
 423 pronounced seasonal ET_o variation, which reduces ratio between data noise and variation. In
 424 CH-Oe2, FR-Gri 2005-2006, DE_Geb 2006-2007, and BE-Lon 2004-2005 sites, a correlation
 425 higher than 0.80 was observed considering outcomes with the HS and PM equations, using
 426 both climate datasets. At these sites, the model accuracy was confirmed by an index of
 427 agreement higher than 85%. As observed by other authors (Allen et al., 1998; Temesgen et al.,
 428 1999; Droogers and Allen, 2002; Martinez-Cob and Tejero, 2004; Alexandris et al., 2008; de
 429 Sousa Lima et al., 2013), an overestimation of ET_o with HS was noticed at sites characterized
 430 by high humidity (Klingenberg, Grignon, Oensingen) characterized by more rainy days. Based
 431 on this finding, the ET_o _PM was used for regional ET_a simulations (Section 3.2).

432
 433 *Tab. 3. Assessment of modelled ET_o computed using Hargreaves (with E-OBS and EI gridded data) and*
 434 *Penman Monteith (EI gridded data) equation against site observations (FLUXNET sites). Values are*
 435 *expressed as a mean of the values estimated in each site and for each available growing season.*
 436

HS_EOBS vs HS_site	HS_EI vs HS_site	PM_EI vs PM_site
<i>RMSE (mm)</i>		
1.74	1.85	1.01
<i>MBE (mm)</i>		
0.86	0.89	-0.03
<i>MAE (mm)</i>		
1.49	1.59	0.79
<i>IA (%)</i>		
59	59	81

437
 438
 439
 440
 441
 442
 443
 444

3.2 SIMETAW_GIS application at Mediterranean scale

SIMETAW_GIS model was applied to estimate ET_c , ET_a , yield, and irrigation requirements for maize, grape, and wheat in the Mediterranean domain for the baseline period (1976-2006) and future period (2036-2065) under RCP 4.5 and 8.5 climate scenarios.

3.2.1 Climate projections for precipitation

445
 446
 447 The most severe impact of climate change on precipitation in Mediterranean countries is
 448 expected under RCP 8.5 (Table 4). Historically, largest precipitations are estimated for the
 449 Balkan countries, with a peak of 1441 mm in Montenegro. The lowest precipitations are
 450 **evaluated** in Libya, Egypt, and Israel showing a general low precipitation regime (Table 4).
 451 Under climate change conditions, precipitation reduction higher than 15% were estimated in
 452 Algeria, Greece, Morocco, and Tunisia under both RCPs and in Libya under RCP 8.5. The
 453 lowest precipitation decrease is expected to occur in France and Israel under RCP 8.5 and in
 454 Cyprus under RCP 4.5 (pcp reduction < - 1%). No changes are projected in Egypt under RCP
 455 4.5. In the other Mediterranean countries, precipitation reduction ranged from 1% to 14%. In
 456 some countries (i.e., Croatia, Egypt, France, and Slovenia with RCP 8.5; Israel and Syria with
 457 RCP 4.5) the projected cumulated precipitation values are higher than in the baseline period
 458 (Table 4).
 459

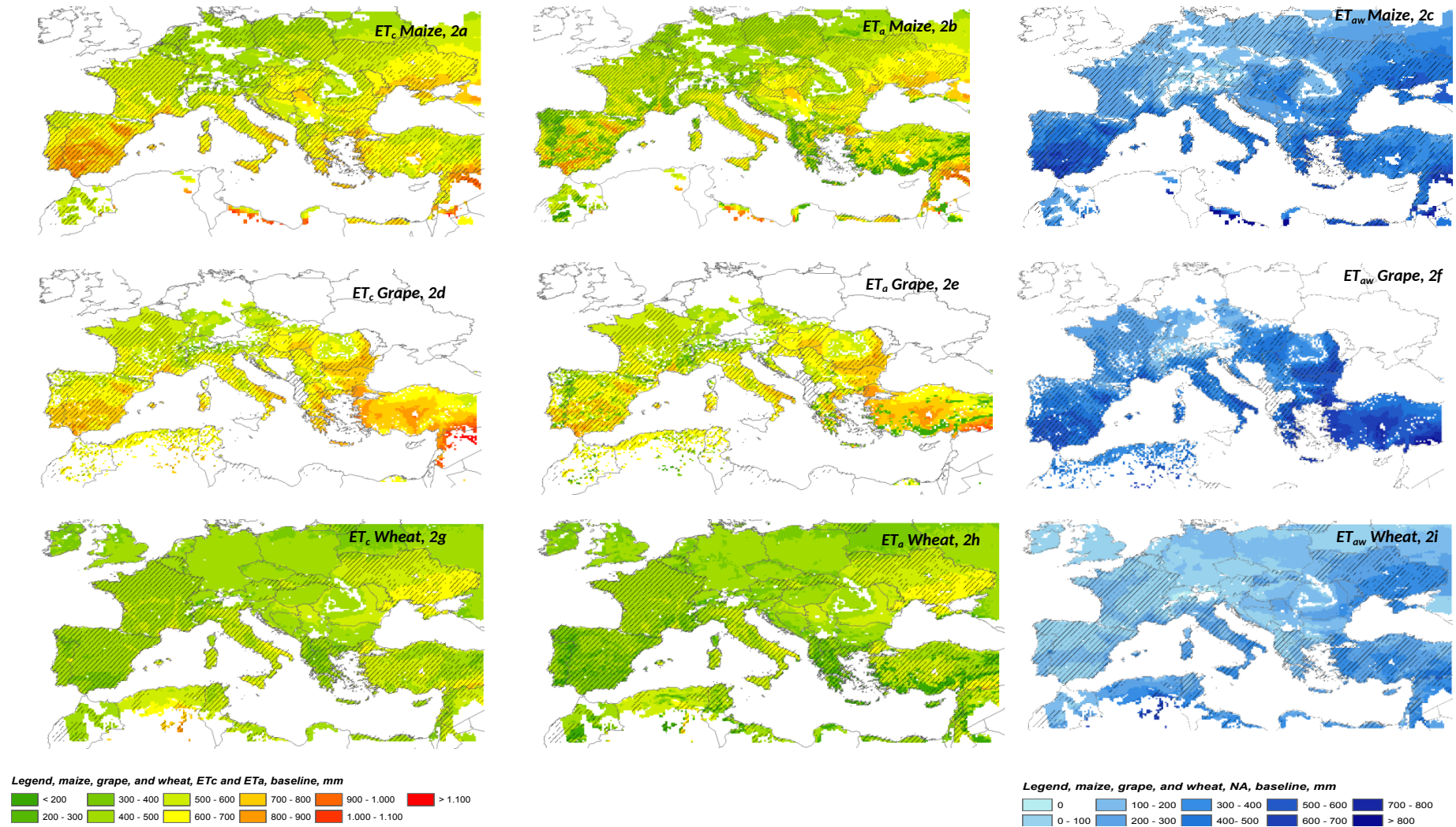
460 *Tab. 4. Precipitation values in the baseline period (pcp bas, mm) and climate anomalies (%) in the*
 461 *Mediterranean Countries for RCP 4.5 and 8.5 scenarios.*

	Algeria	Albania	Bosnia and Herzegovina	Cyprus	Croatia	Egypt	France	Greece	Israel	Italy
pcp bas	185	1095	1026	165	895	38	882	521	134	834
pcp45-bas	-15.75	-9.56	-7.45	-0.62	-4.66	0	-2.97	-18.35	5.65	-7.52
pcp85-bas	-26.08	-6.39	-5.65	-12.37	1.08	5.29	0.12	-16.21	-0.96	-7.54
	Lebanon	Libya	Morocco	Montenegro	Slovenia	Spain	Syria	Tunisia	Turkey	
pcp bas	397	76	352	1441	1084	711	146	163	479	
pcp45-bas	-3.08	-13.21	-19.01	-9.53	-2.61	-10.48	4.3	-15.9	-6.35	
pcp85-bas	-14.33	-22.79	-27.49	-4.81	5.5	-6	-6.43	-28.7	-8.52	

462
 463
 464
 465
 466
 467
 468
 469
 470
 471
 472
 473
 474
 475
 476
 477

3.3.2 Impact of climate change on crop water consumption and irrigation requirement

Regional baseline values for maize, grape, and wheat ET_c , ET_a , and ET_{aw} are shown in Figure 2 for the Mediterranean domain and discussed for each crop in the next sections. The estimated actual evapotranspiration (Figures 2b, 2e, 2h) is lower than the crop water consumption (Figures 2a, 2d, and 2g), highlighting a water stress coefficient $K_s < 1$ within the study areas, with consequent yield losses (Figure 3). This is most likely related to the pedo-climatic (climate, maximum soil depth, soil water holding capacity, and maximum rooting depth) conditions and management practices, i.e., assumptions about (1) the percentage of full water allocation applied, (2) planted area, (3) irrigation system, and (4) allowable depletion.



479 Fig. 2. Regional mean of ET_c (2a, 2d, 2g), ET_a (2b, 2e, and 2h) and ET_{aw} (2c, 2f, and 2i) for maize, grape and wheat during 1976-2005 considering potential
 480 crop distribution widespread in the entire domain. The effective crop irrigated areas are distinguished using solid diagonal lines.

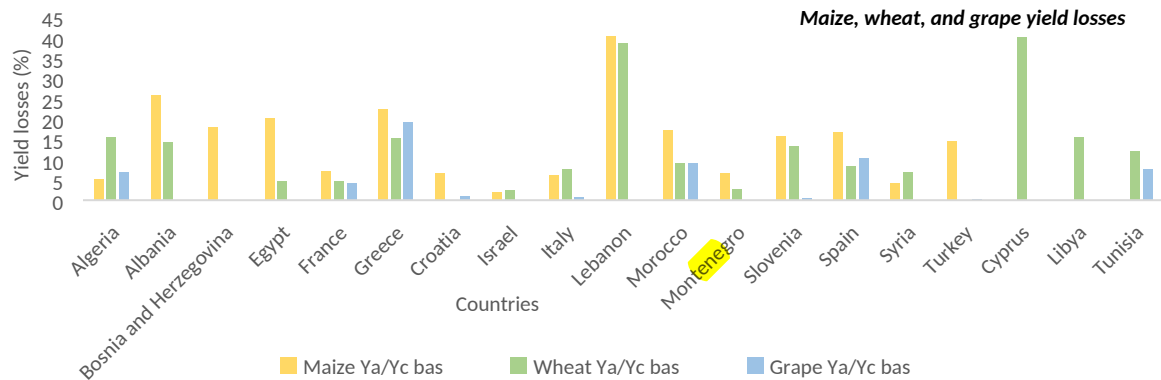


Fig. 3. Regional mean yield responses to water deficit (Y_d/Y_c) for maize, grape and wheat during 1976-2005.

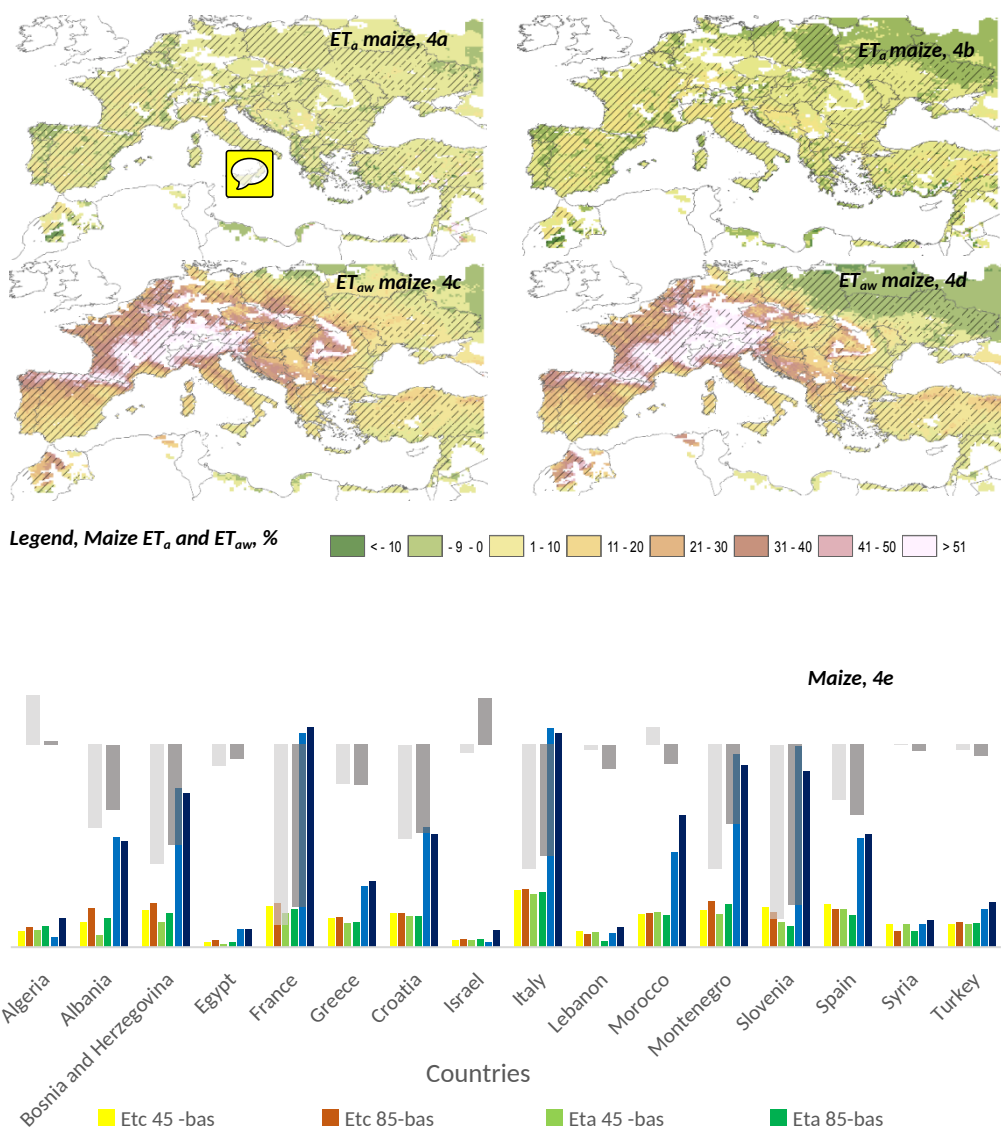
3.3.2.1 Maize

The Mediterranean region baseline crop evapotranspiration estimated for maize under optimal water supply on a country average varied in a range from 533 mm (Morocco) to 893 mm (Algeria) (Figure 2a). Under climate change, an overall increase of ET_c was foreseen. High rates of change (increase of 5-6%) were observed in most Balkan countries. The most severe impact of climate change was found in Italy where future maize water consumption increase, under both RCPs, by about 7-8% (Figure 4e). In general, the largest changes were estimated under RCP8.5, except for Spain and Syria. Slight differences between the two climate scenarios were estimated. The trend of ET_a is the same as ET_c but, due to stress conditions, the values estimated for ET_a in 2036-2065 were slightly lower than ET_c (1-2%) (Figures 4a, 4b, 4e).

The evapotranspiration of applied water (ET_{aw}) within the baseline period ranged from 210 mm (Slovenia) to 769 mm (Algeria) (Figure 2c). In most countries, the changes in ET_{aw} follow the precipitation variability under the two scenarios (Table 4). A future increase in irrigation demand was observed in all Mediterranean countries, with peaks of 25-28% found in France, Italy, Slovenia, and Montenegro. The lowest increase of crop water demand (1-6%) was estimated under RCP4.5 in Algeria, Israel, Egypt, Lebanon, Syria, and Turkey. Irrigation demand was expected to increase from about 14-17% in Morocco, Spain, Croatia and Albania (Figures 4c, 4d, 4e).

Despite maize being irrigated both during baseline and future periods, water applications were not completely adequate to fully satisfy crop water needs, causing a limited water stress, which led to yield losses (Figure 3 and 4e). The highest difference of yield losses between future and past values were estimated in France, Italy, Slovenia, Bosnia and Herzegovina, and Montenegro. The lowest changes were estimated in Turkey (RCP 4.5) and Syria (both RCPs). Maize production was found to be higher (i.e. lower losses) under climate change in Algeria, Israel (RCP 8.5), and Morocco (RCP 4.5) (Figure 4e).

In general, a trend of maize yield reduction is in line with Giannakopoulos et al. (2005), Gallo (2015), and Tubiello et al., (2000). The impact of climate change on future ET_c , ET_a and ET_{aw} for maize in the Mediterranean countries, under both RCPs, is expected to be on average about 4%, 3%, and 13% higher than the baseline, respectively. The trend for increasing maize water requirement from Northern to Southern Italy under both RCP 4.5 and 8.5 scenarios is in line with Gallo (2015). An increase between 7% and 9% of maize irrigation requirement under the 5°C climate trajectory was estimated by Fader et al. (2016) in Mediterranean countries. Furthermore, an increase of maize ET_{aw} of 35% was found by Kapur et al. (2007) under climate change conditions. Lower change (increase of 5%) was estimated by Mancosu (2013) for maize cultivated in Sardinia (Italy). Increasing irrigation needs of spring-summer crops were also projected by Lovelli et al. (2010).



523 Fig. 4. Rate of change of ET_a (4a. ET_a 45-bas, 4b. ET_a 85-bas) and ET_{aw} (4c. ET_{aw} 45-bas, 4d. ET_{aw} 85-
 524 bas) values weighted for the irrigated maize distribution between future climate condition (2036-2065)
 525 under both RCP 4.5 and 8.5 scenarios, and the baseline (1976-2005) for the entire domain with a focus
 526 on the Mediterranean countries (Fig. 4e). Rate of changes of maize ET_c (ET_c 45-bas, ET_c 85-bas) and
 527 yield losses (Y_a/Y_c 45-bas, Y_a/Y_c 85-bas) between future and baseline period in the Mediterranean
 528 countries are shown in figure 4e.

529
530

531 **3.3.2.2 Grape**

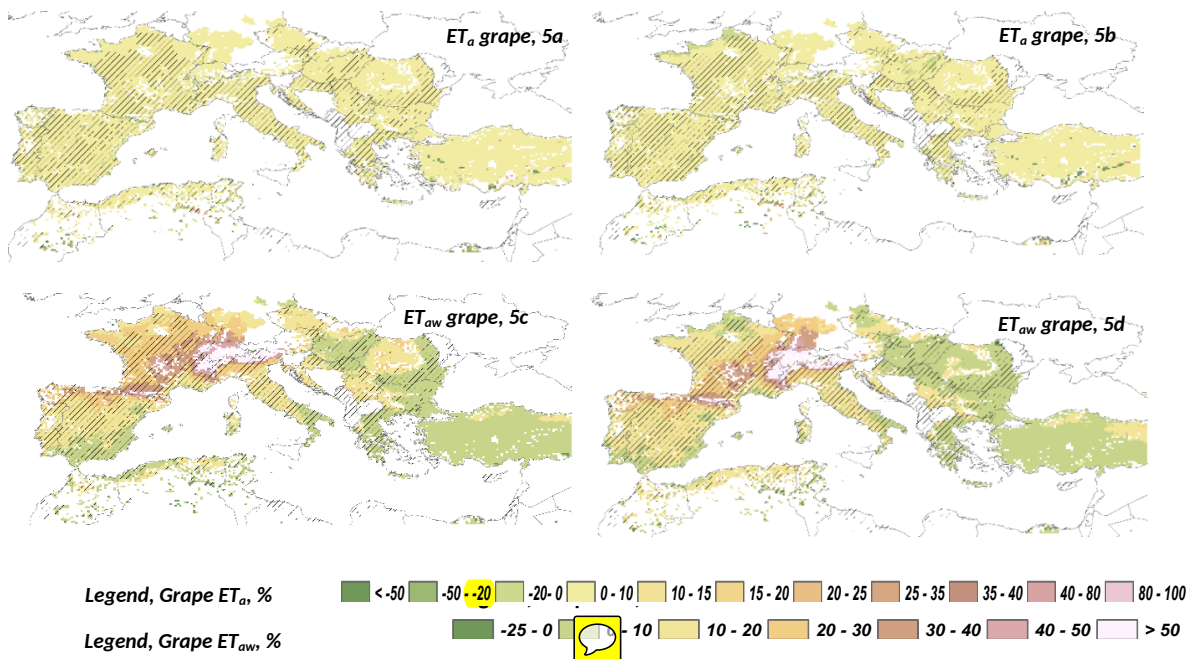
532 The greatest average crop water consumption in the baseline was estimated in Turkey (888
 533 mm), with the lowest in Slovenia (570 mm). Values between 700 and 800 mm were found in
 534 Spain and Greece, and between 600 mm and 700 mm in all other Mediterranean countries
 535 (Figure 2d). Under climate change conditions, a mean increase (3%) of crop evapotranspiration
 536 was expected in the Mediterranean countries with peaks (~ 6%) in France and Italy under the
 537 RCP 4.5 scenario. The crop water consumption estimated under RCP 8.5 was slightly lower (-
 538 0.70% on average) than under RCP 4.5 in France, Croatia, Italy, Slovenia, Spain, and Turkey.
 539 During the baseline, the trend of ET_a was the same as that estimated for ET_c (Figure 2e).

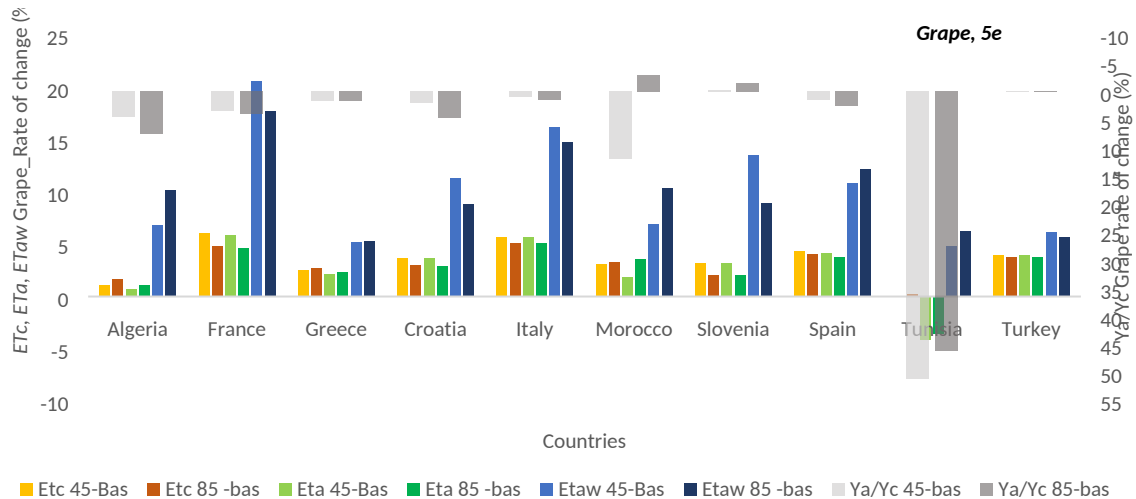
540 Although actual grape water consumption tending to rise in all countries, they were still lower
 541 than full crop water requirements (optimal water irrigation supply), except for Turkey where
 542 no relevant difference was found. A reverse trend was shown in Tunisia where the ET_a values
 543 were $\sim 4\%$ lower than in the baseline (Figure 5e). The highest yield reduction occurs in Greece
 544 (19%), Morocco and Spain (10%) while the lowest in Italy and Croatia (1%) (Figure 3). No
 545 changes between future and past yield losses happen in Turkey under both RCPs and Slovenia
 546 under RCP 8.5. Under RCP 4.5, the yield losses in Morocco and Slovenia are slightly lower
 547 than during the baseline ($\sim 2\text{-}3\%$). The peak of future yield reduction is projected for Tunisia
 548 under both RCPs with losses up to 51% (RCP 4.5). Using different meteorological gridded
 549 input data, Moriondo et al. (2011) projected a decrease in future yield in Tuscany (Italy). Ferrise
 550 et al. (2016) attribute the negative impact of increasing temperature and precipitation reduction
 551 on grape yield in the Mediterranean basin to shorter phenological growth periods.

552 As for ET_c and ET_a , the highest irrigation demand (ET_{aw}) in the baseline occurs in
 553 Turkey (706 mm) and the lowest in Slovenia (289 mm). A peak of about 600 mm was found
 554 in Greece, followed by Tunisia and Spain, where values between 400 mm and 500 mm are
 555 reported. Lower values (400-500 mm) occur in Italy, Algeria, France, Croatia, and Morocco
 556 (Figure 2f). In general, the grape irrigation demand (ET_{aw}) followed precipitation patterns
 557 (Table 4). The largest increase of irrigation requirement, under both RCPs, is expected in
 558 France ($\sim 19\%$) and Italy ($\sim 15\%$) followed by Slovenia, Croatia, and Spain ($\sim 11\%$). Changes
 559 no higher than $\sim 6\%$ are predicted for Tunisia, Greece, and Turkey (Figure 5c, 5d, 5e).

560 A focus on the Mediterranean Countries shows a mean ET_{aw} value about **10 %** higher
 561 in the future under both RCPs. Although grape is usually cultivated under rainfed conditions
 562 in Sardinia region, the ET_{aw} is expected to increase by about 6% with climate change (Mancosu,
 563 2013).

564
565
566
567





568 Fig. 5. Rate of change of ET_a (5a. ET_a 45-bas, 5b. ET_a 85-bas) and ET_{aw} (5c. ET_{aw} 45-bas, 5d. ET_{aw} 85-
569 bas) values weighted for the irrigated grape distribution between future climate condition (2036-2065)
570 under both RCP 4.5 and 8.5 scenarios, and the baseline (1976-2005) for the entire domain with a focus
571 on the Mediterranean countries (Fig. 5e). Rate of changes of maize ET_c (ET_c 45-bas, ET_c 85-bas) and
572 yield losses (Y_a/Y_c 45-bas, Y_a/Y_c 85-bas) between future and baseline period in the Mediterranean
573 countries are shown in figure 5e.

574

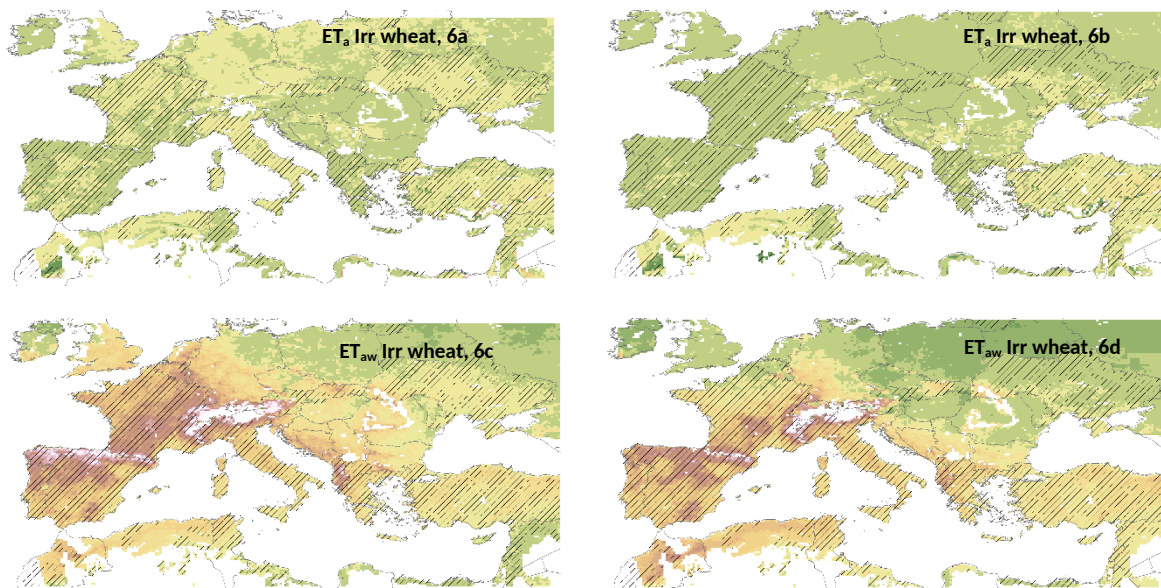
575 3.3.2.3 Irrigated wheat

576 Although wheat is generally cultivated under rainfed conditions, there are some irrigated areas
577 concentrated in the Mediterranean basin. The trend of wheat evapotranspiration for the baseline
578 period estimated in this work is in line with Saadi et al. (2014), even if two different approaches
579 were adopted. Yield losses over Mediterranean countries are estimated as the difference
580 between ET_c and ET_a values. Losses up to 40% are shown for Cyprus and Lebanon during the
581 baseline period (Figure 3). Under climate change, the highest difference between future and
582 past climate are estimated for Albania, France, Montenegro and Spain ($Y_a/Y_c > 20\%$), while
583 lower losses are predicted in Egypt (both RCPs) and Israel (RCP 4.5). These trends are in line
584 with Saadi et al. (2014) and in contrast with Moriondo et al. (2011) who project an increase of
585 not irrigated winter wheat yield in the same area. In this analysis, ET_c values ranged from 409
586 to 631 mm (Figure 2g), where the lowest and the highest values are 100 mm higher and 233
587 mm lower, respectively, than the values estimated by Saadi et al. (2014). The highest mean
588 difference of wheat water consumption is estimated for Morocco (increase of $\sim 4\%$) under both
589 RCPs. Negative ET_c rate of change values are expected in Albania, Libya, and Tunisia under
590 both RCPs and in Egypt, France, Slovenia, and Spain under RCP 8.5. In these countries, the
591 ET_c values predicted under future climate conditions are lower than the ones estimated in the
592 baseline (Figures 6a, 6b, 6e). In the baseline, ET_a values range from 525 mm (Italy) to 277 mm
593 (Cyprus) (Figure 2h). In several countries (Figures 6a, 6b, 6e), under climate change
594 conditions, the values of ET_a increased relative to the baseline. Indeed, negative changes
595 between future and baseline ET_a values countries with peak of -5% and -4% are expected in
596 Albania, under RCP 4.5, and in Spain, under RCP 8.5.

597 Figure 2i shows crop irrigation requirement values lower than 100 mm in Albania,
598 France, Montenegro, and Spain. The highest applied water demand in the baseline is reported
599 for Syria and Turkey (304 mm). Irrigation demand under climate change is expected to slightly
600 decrease in Egypt under both RCPs while in Israel, Lebanon, and Syria only under RCP 4.5. A
601 noticeable increase ($\sim 40 - 46\%$) of wheat irrigation demand under climate change is projected
602 for France, Spain, Montenegro, and Albania under RCP 4.5. As a result of slightly higher

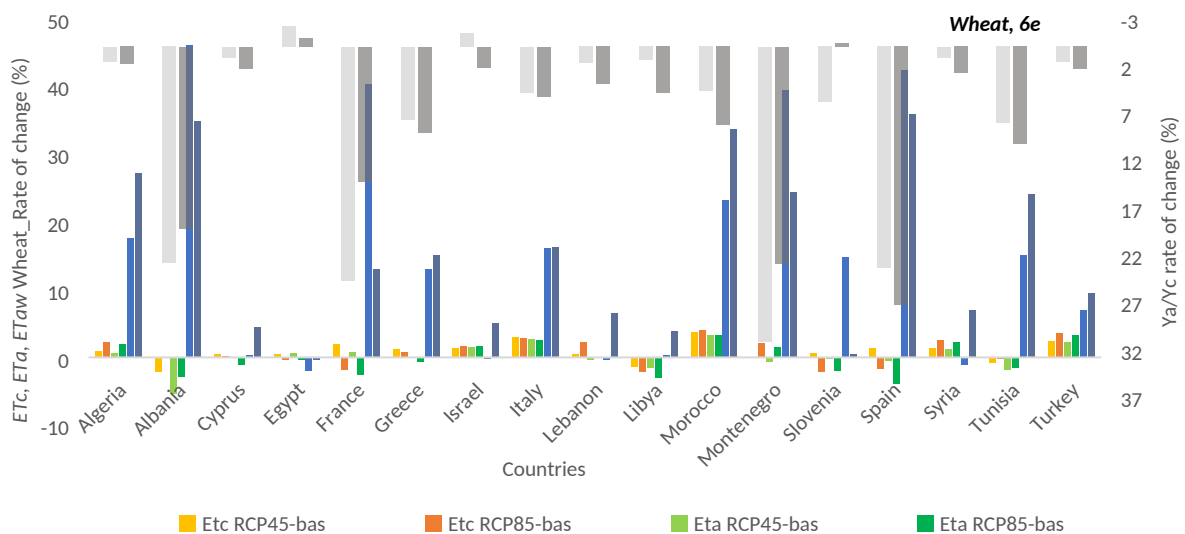
603 precipitation under RCP 8.5 compared to RCP 4.5 (Table 4), in the same countries lower ET_{aw}
 604 values were found under RCP 8.5 (Figures 6c and 6d). The highest difference between the two
 605 climate scenarios arises in France (27%) with the lowest in Italy (0.16%). Considering a
 606 doubling of atmospheric CO_2 concentration, wheat ET_a values are expected to decrease by
 607 about 28 % (CGM2 data) 8 % (RCM data) in the period 2070-2079 in Turkey according to
 608 Yano et al. (2007). While increasing ET_c values are projected in this work, decreasing ET_c , in
 609 no-stress conditions, are reported in Saadi et al. (2014) and Supit et al. (2010). They attribute
 610 the change in ET_c to a shorter growing season. The negative impact of climate change, i.e. the
 611 increase of wheat net water application is in agreement with other studies (Tubiello et al., 2000;
 612 Yano et al., 2007; Özdoğan, 2011; Saadi et al., 2014; Valizadeh et al., 2014). In contrast, in
 613 Southern Italy in 2071, Lovelli et al., (2010) state that no significant ET_{aw} increase in autumn-
 614 winter crops is anticipated, while increasing ET_{aw} is expected for spring-summer crops.

615
616



617 Legend, Irr Wheat ET_a and ET_{aw} , %

618
619



620

621 *Fig. 6. Rate of change of ET_a (6a. RCP45-bas, 6b. RCP85-bas) and ET_{aw} (6c. RCP45-bas, 6d. RCP85-*
622 *bas) values weighted for the irrigated wheat distribution between future climate condition (2036-2065)*
623 *under both RCP 4.5 and 8.5 scenarios, and the baseline (1976-2005) with a focus on the Mediterranean*
624 *countries (Fig. 6e). Rate of changes of wheat yield losses between future and baseline period are shown*
625 *in figure 6e.*

626

627 **4 Discussion**

628

629 The findings show an overall reduction of projected precipitation in Southern Mediterranean
630 countries which, in line with Keuler et al. (2016), is in general greater under RCP 8.5. The
631 simulated reference, crop, and actual evapotranspiration, as well as irrigation requirement are
632 projected to increase under future climate conditions, and often differences between future and
633 past climate conditions are greater under the RCP 4.5 scenario. On average, the maize and
634 grape crop water consumption in the Mediterranean countries is expected to increase on
635 average ~ 3-4% under both RCPs, with the most consistent increases in Italy (~ 7% under both
636 RCPs) and in France (~ 6% under RCP 4.5). Lower values are projected for wheat which is
637 expected to consume on average ~ 0.5% more under climate change conditions with peak of ~
638 4% in Morocco.

639 Generally, under both RCPs, the rate of change of maize, wheat, and grape water
640 consumption under deficit water and non-optimal pedo-climatic conditions (ET_a) are on
641 average lower than in well watered conditions. In Mediterranean countries, maize, wheat, and
642 grape production will require on average about 13%, 16%, and 10% more applied water under
643 climate change conditions, respectively. The amount of water applied to satisfy grape needs in
644 the future decades is higher in relevant wine producing countries such as France (~19%), Italy
645 (15%), and Spain (11%) than in other Mediterranean countries. Rates of change are particularly
646 high in the southern part of these countries (Figure 5c and 5d), where conflicts on water use
647 and less favorable conditions could lead to impact on crop productivity. Yet, a high quality
648 wine production may be enhanced. The lowest impact of climate change on grape irrigation
649 demand is expected in Turkey, Tunisia, and Greece (increase of ~ 6%). A future increase of
650 applied water between ~ 20% – 29% is expected for maize production in Bosnia and
651 Herzegovina, France, Italy, Slovenia and Montenegro due to reduced precipitation during
652 2036-2065 (Table 4). In France, Albania, Spain, and Morocco the wheat irrigation is estimated
653 to increase under climate change by more than ~ 40% under RCP 4.5. In general, Egypt, Israel,
654 and Lebanon show the least change for maize water needs (ET_{aw} increase < ~ 3% under both
655 RCPs), whereas the lowest wheat water applications are needed in Cyprus, Egypt, Israel, Libya,
656 and Syria ($-2\% < ET_{aw} < 0\%$ under RCP 4.5).

657 Although irrigation application is practiced, the ET_a estimated was in general lower
658 than ET_c due to the pedoclimatic conditions and management practices assumed in this work.
659 Assuming no changes in input data, actual evapotranspiration values may increase changing
660 the frequency and number of irrigation events (AD < 50%). This management strategy can
661 reduce water stress (but increase water demand) therefore increasing ET_a , which in turn reduces
662 yield losses. It is worth noting that, in this case, much water may be applied for the crop growth,
663 and an environmental-economic analysis could help in achieving the best balance between the
664 impact on water resources and yield losses. In addition, the price of water should be taken into
665 account, since it impacts farm business.

666 This work is in line with several studies investigating crop water consumption and
667 irrigation requirements using models at different scales and at different resolutions, and
668 considering different scenarios. Keeping a focus on Mediterranean irrigated agriculture, this
669 study agrees with an expected increase in crop water needs due to increasing drought risk which

670 is expected to characterize Southern Countries in the near future (Rodriguez-Diaz et al., 2007;
671 Saadi et al., 2014; Tanasijevic et al., 2014; Fader et al., 2015; Fader et al., 2016).

672 Irrigation practices are exacerbated in Mediterranean regions due to the projected
673 warmer and drier summer months when the amount of agricultural water is constrained due to
674 other sectors' water needs. Tourism is a critical economic sector, but also demands considerable
675 drinking water and water for leisure facilities leading to increased conflicts among sectors for
676 water use. Uncontrolled water abstraction may exacerbate the water security issues by creating
677 imbalances between water supply and demand (Collins, 2009). Such inter-sectoral water-
678 related issues could hamper efforts throughout the region in achieving **SDG6 goals**. This work
679 further highlights the potential severity of increases in water-related issues in the
680 Mediterranean, related to both expected supply decline and demand increase. Unfortunately,
681 in this region water security challenges are not the only issue to be confronted regarding
682 agricultural production.

683 **This work suggests widespread crop yield declines resulting from water shortages,**
684 **especially for food-supply crops such as maize and wheat.** As aforementioned, despite the crops
685 being irrigated, the study shows that water applications are inadequate to fully satisfy crop
686 water needs, resulting in a stress coefficient $K_s < 1$ and consequent crop yield reductions. In
687 Mediterranean countries, the beneficial effect of future increasing atmospheric CO₂
688 concentration on yield losses is more evident on grape and wheat, with yield losses limited to
689 about 8%, while for maize yield losses can reach about 13%. Grape yield losses are possibly
690 related to increasing temperature effects on the length of the growing season (Ferrise et al.,
691 2016). Although C3 plants, i.e., wheat and grape, may benefit from increasing levels of
692 atmospheric CO₂ due to their physiology (Patterson et al., 1984; Cure and Acok, 1986), this
693 positive effect may be threatened by other factors such as the changes in precipitation
694 frequency and intensity, which can lead to negative effects on crop production (IPCC, 2007),
695 particularly in areas where water resources are scarce.

696 In the near future, non-irrigated crop production in southern Europe is expected to
697 decrease by about 50%, and this may lead to climate change induced crop abandonment (EEA,
698 2019). Decreases in crop yield and the abandonment of productive land could threaten local,
699 regional, and European food security, which led to the global challenge to achieve the
700 **Sustainable Development Goals 2** (SDG 2) in the Mediterranean basin (SDSN, 2019).
701 Furthermore, unsustainable agriculture may lead to an increase in food imports, with a
702 consequent increase in food prices and food supply vulnerability. It can cause lower and/or less
703 stable income for farmers with an unavoidable impact on the agricultural sector. Taken
704 together, the potential for agricultural water demand leading to increased water competition
705 and threats to water supply, and the expected decreases in crop yields partly due to water and
706 climate impacts, strongly suggest that increasing the resilience of agricultural sector to extreme
707 events in Mediterranean countries is a critical priority from local to European governments in
708 terms of managing water consumption (SDG6) while also maintaining crop production
709 (SDG2).

710 The first step to cope with these issues is to increase knowledge about the water
711 consumption and irrigation requirements of Mediterranean crops to better manage water
712 resources, as well as better understanding of yield declines, particularly in regions already
713 largely affected by water scarcity and a multitude of water-demanding sectors. This study
714 further contributes to such knowledge. Although the adaptation of the agricultural sector to

715 climate change is progressing, the process needs to be accelerated. Policies targeted to facilitate
716 and speed up this transition at different time and spatial scales should be addressed by decision
717 makers faster and better (EEA, 2019).

718 Some limitations in this study will be addressed in future work, such as: (i) changes in
719 crop breeding, new cultural practices and technologies, and shifts in sowing, bud break, and
720 harvest date, which may have an impact on crop adaptation to climate change conditions, (ii)
721 changes in the percentage of cultivated areas due to climate or anthropogenic factors, (iii)
722 evaluation of more crops under several water management scenarios, (iv) availability of higher
723 resolution input gridded data to include more details in the outcomes at Mediterranean scale,
724 and (v) use of climate models ensemble to reduce result uncertainties, and, model biases.

725

726

727 **5 Conclusions**

728 In this work, the Simulation of Evapotranspiration of Applied Water (SIMETAW#) model was
729 implemented in two new versions able to simulate crop water consumption and irrigation
730 demand at both local (SIMETAW_R) and regional scale (SIMETAW_GIS) according to the
731 stakeholder's needs. SIMETAW# model was converted and implemented in R programming
732 language.

733 SIMETAW_R was validated in ten experimental sites, and the SIMETAW_GIS performance
734 in Mediterranean countries was assessed by estimating the impact of climate change on maize,
735 wheat, and grape water consumption and irrigation requirements for the baseline (1976-2005)
736 and the future climate conditions (2036-2065), under RCP 4.5 and 8.5 scenarios.

737 SIMETAW_R performed well at the local level. Estimated increases in crop water
738 needs under future climate conditions in Mediterranean Countries are predicted. Irrigation
739 demand increases were often greater under RCP 4.5 than 8.5 scenario. Crop yields are also
740 expected to decline in many southern Mediterranean countries. The increased water demand
741 and decreasing crop yields pose dual challenges for local to European agricultural policy
742 regarding efforts towards achieving goals in SDG2 and SDG6. The SIMETAW_R model
743 outcomes at local scale as well as the SIMETAW_GIS platform gridded outcomes at regional
744 scale contribute to increase awareness on climate change issues regarding crop water
745 consumption and irrigation requirements and agricultural production in Mediterranean regions.
746 To tackle climate change impact on the agricultural sector, adaptation strategies should be
747 developed, supported, and implemented. In view of the rapid demographic growth and the
748 consequent food security issue, it is necessary to cope with climate change through strategies
749 targeted to achieve agricultural sustainable production. In this context, this study adds useful
750 information to better inform such policy decisions surrounding agricultural practices and crop
751 water management both at local and regional scale.

752

753 **Acknowledgements**

754 This research was funded by the Autonomous Region of Sardinia (P.O.R., Regional
755 Operational Programme) and by funds for research (2019) from University of Sassari. The
756 work was developed within the Ph.D program in Agrometeorology and Ecophysiology of
757 Agricultural and Forestry Ecosystems at the University of Sassari in collaboration with the IHE
758 Delft Institute for Water Education. The authors acknowledge the principal investigators of the
759 FLUXNET sites who kindly provided data and information.

760 **References**

- 761 Alexandris, S., Stricevic, R., Petkovic, S., 2008. Comparative analysis of reference
762 evapotranspiration from the surface of rainfed grass in central Serbia, calculated by six
763 empirical methods against the Penman-Monteith formula. European Water
764 Publications 21/22, 17-28.
- 765 Allen, R.G., Pereira, L.S., Raes, D., Smith, M., 1998. Crop evapotranspiration: Guidelines for
766 computing crop requirements. Irrigation and Drainage Paper No. 56, FAO, (56), 300,
767 <https://doi.org/10.1016/j.eja.2010.12.001>.
- 768
- 769 Allen, R.G., Walter, I.A., Elliott, R.L., Howell, T.A., Itenfisu, D., Jensen, M.E., Snyder,
770 R.L., 2005. The ASCE Standardized Reference Evapotranspiration Equation.
771 American Society of Civil Engineers, Reston, VA.
- 772
- 773 Allen, R.G., Pruitt, W.O., Wright, J.L., Howell, T.A., Ventura, F., Snyder, R.L.,
774 Itenfisu, D., Steduto, P., Berengena, J., Yrisarry, J.B., Smith, M., Pereira, L.S.,
775 Raes, D., Perrier, A., Alves, I., Walter, I., Elliott, R.A., 2006. Recommendation
776 on standardized surface resistance for hourly calculation of reference ETo by the
777 FAO56 Penman–Monteith method. Agricultural Water Management 81 (1–2),
778 1–22.
- 779
- 780 Anderson, J., Dimou, P., Jones, G.V., Kalivas, D., Koufos, G., Mavromatis, T., Koundouras,
781 S., Fyllas, N.M., 2014. Harvest Dates, Climate, And Viticultural Region Zoning In
782 Greece, [https://inside.sou.edu/assets/bce/Anderson_etal_Greece_Terroir_Congress_20](https://inside.sou.edu/assets/bce/Anderson_etal_Greece_Terroir_Congress_2014.pdf)
783 14.pdf.
- 784 Andreini, L., Viti, R., Scalabrelli, G., 2009. Study on the morphological evolution of bud break
785 in *Vitisvinifera* L. Vitis 48, No.4, 153–158.
- 786 Baldocchi, D.D., Hincks, B.B., Meyers, T.P., 1988. Measuring biosphere-atmosphere
787 exchanges of biologically related gases with micrometeorological methods. Ecology
788 69, No. 5.
- 789
- 790 Bao, Y.W., Hoogenboom, G., McClendon, R., Vellidis, G., 2017. A comparison of the
791 performance of the CSM-CERES-Maize and EPIC models using maize variety trial
792 data. Agric. Syst. 150, 109–119.
- 793
- 794 Batjes, N.H., 2000. Global Data Set of Derived Soil Properties, 0.5-Degree Grid (ISRIC-
795 WISE). Global Data Set of Derived Soil Properties, 0.5-Degree Grid (International Soil
796 Reference and Information Centre - World Inventory of Soil Emission Potentials). Data
797 set. Available on-line <http://www.daac.ornl.gov>. From Oak Ridge National Laboratory
798 Distributed Active Archive Center, Oak Ridge, Tennessee, U.S.A.,
799 doi:10.3334/ORNLDAAAC/546.
- 800
- 801 Brooks, J., (ed.) 2012. Agricultural Policies for Poverty Reduction, OECD Publishing, Paris,
802 <https://doi.org/10.1787/9789264112902-en>.
- 803

- 804 Burba, G., 2013. Eddy covariance method for scientific, industrial, agricultural and regulatory
805 applications: A field book on measuring ecosystem gas exchange and areal emission
806 rates: LI-Cor Biosciences.
807
- 808 Camps, J.O., Ramos, M.C., 2012. Grape harvest and yield responses to inter-annual changes
809 in temperature and precipitation in an area of north-east Spain with a
810 Mediterranean climate. *International Journal of Biometeorology* 56, 853–864,
811 doi:10.1007/s00484-011-0489-3.
812
- 813 Christoph, N., Rossmann, A., Voerkelius, S., 2003. Possibilities and limitations of wine
814 authentication using stable isotope and meteorological data, data banks and statistical
815 tests. Part 1: Wines from Franconia and lake Constance 1992 to 2001.
816 *Mitteilungen Klosterneuburg* 53, 23-40.
817
- 818 Collins, 2009. Water scarcity and drought in the Mediterranean. *Water scarcity and drought in*
819 *the Mediterranean.*
820
- 821 Cortesi, P., Bisiach, M., Ricciolini, M., Gadoury, D.M., 1997. Cleistothecia of
822 *Uncinulanecator*. An additional source of inoculum in Italian vineyards. *Plant Disease*
823 81, 922-926.
824
- 825 Cramer, W., Guiot, J., Fader, M., et al., 2018. Climate change and interconnected risks to
826 sustainable development in the Mediterranean. *Nature Clim Change* 8, 972–980,
827 doi:10.1038/s41558-018-0299-2.
828
- 829 Cure, J. D., Acock, B., 1986. Crop responses to carbon dioxide doubling: a literature
830 survey. *Agricultural and Forest Meteorology* 38, 127-145.
831
- 832 Dee, D., Uppala, S.M., Simmons, A.J., Berrisford, P., Poli, P., Kobayashi, S., Andrae, U.,
833 Balsameda, M.A., Balsamo, G., Bauer, P., Bechtold, P., Beljaars, A.C.M., van de Berg,
834 L., Bidlot, J., Bormann, N., Delsol, C., Dragani, R., Fuentes, M., Geer, A.J.,
835 Haimberger, L., Healy, S.B., Hers-bach, H., Holm, E.V., Isaksen, L., Kallberg, P.,
836 Kohler, M., Matricardi, M., McNally, A.P., Monge-Sanz, B.M., Morcrette, J.J., Park,
837 B.K., Peubey, C., de Rosnay, P., Tavolato, C., Thepaut, J.N., Vitart, F., 2011. The era-
838 interim re-analysis: configuration and performance of the data assimilation system.
839 *Quarterly Journal of Royal Meteorological Society* 137, 553–597.
840
- 841 Droogers, P., Allen, R.G., 2002. Estimating reference evapotranspiration under inaccurate data
842 conditions. *Irrigation and Drainage Systems* 16, 33–45. Kluwer Academic Publishers.
843 Printed in the Netherlands.
- 844 EEA, 2019. Climate change threatens future of farming in Europe.
845 <https://www.eea.europa.eu/highlights/climate-change-threatens-future-of>.
846
- 847 Elliott, J., Müller, C., Deryng, D., Chryssanthacopoulos, J., Boote, K.J., Büchner, M., Foster,
848 I., Glotter, M., Heinke, J., Iizumi, T., Izaurralde, R.C., Mueller, N.D., Ray, D.K.,
849 Rosenzweig, C., Ruane, A.C., Sheffield, J., 2015. The Global Gridded Crop Model
850 Intercomparison: data and modeling protocols for Phase 1 (v1.0). *Geoscientific Model*
851 *Development* 8, 261–277, doi:10.5194/gmd-8-261-2015. www.geosci-model
852 dev.net/8/261/2015/.

853
854 Ezzhaouani, A., Valancogne, C., Pieri, P., Amalak, T., Gaudillère, J., 2007. Water economy by
855 Italia grapevines under different irrigation treatments in a Mediterranean climate.
856 International Journal of Vine and Wine Sciences 41 (3), 131-139.
857
858 Fader, M., von Bloh, W., Shi, S., Bondeau, A., Cramer, W., 2015. Modelling Mediterranean
859 agro- ecosystems by including agricultural trees in the LPJmL model. Geoscientific
860 Model Development 8, 3545–3561, doi:10.5194/gmd-8-3545-2015.
861
862 Fader, M., Shi, S., von Bloh, W., Bondeau, A., Cramer, W., 2016. Mediterranean irrigation
863 under climate change: more efficient irrigation needed to compensate for increases in
864 irrigation water requirements. Hydrology and Earth System Sciences 20, 953–973,
865 doi:10.5194/hess-20-953-2016.
866
867 Falge, E., Baldocchi, D., Olson, R.J., Anthoni, P., Aubinet, M., Bernhofer, C., Burba, G.,
868 Ceulemans, R., Clement, R., Dolman, H., Granier, A., Gross, P., Grunwald, T.,
869 Hollinger, D., Jensen, N.O., Katul, G., Keronen, P., Kowalski, A., Lai, C.T., Law, B.E.,
870 Meyers, T., Moncrieff, J., Moors, E., Suyker, A., Tenhunen, J., Tu, K., Verma, S.,
871 Vesala, T., Wilson, K., Wofsy, S., 2001. Gap filling strategies for long term
872 energy flux data sets. Agricultural and Forest Meteorology 107, 71–77.
873
874 Ferragina, E., Canitano, G., 2014. Water and Food Security in the Arab Countries: National
875 and Regional Implications. Global Environment.
876 <https://doi.org/10.3197/ge.2014.070204>.
877
878 Ferrise, R., Trombi, G., Moriondo, M., and Bindi, M., 2016. Climate change and grapevines:
879 A simulation study for the Mediterranean basin. Journal of Wine Economics,
880 11(1),88–104.
881
882 Gallo, A., 2015. Assessment of the Climate Change Impact and Adaptation Strategies
883 on Italian Cereal Production using High Resolution Climate Data. Ph.D. thesis.
884 University of Sassari.
885
886 Giannakopoulos, C., Bindi, M., Moriondo, M., Le Sager, P., Tin, T., 2005. Climate change
887 impacts in the Mediterranean resulting from a 2 °C global temperature rise. WWF
888 report. Gland, Switzerland, World Wide Fund for Nature.
889
890 Giorgi, F., 2006. Climate change hot-spots, Geophys. Res. Lett., 33, L08707.
891
892 Gualdi, S., Somot, S., Li, L., Artale, V., Adani, M., et al., 2013. The CIRCE simulations:
893 Regional Climate Change Projections with Realistic Representation of the
894 Mediterranean Sea. Bull. Amer. Meteor. Soc., 94, 65-81.
895
896 Guerra, E., Ventura, F., Spano, D., Snyder, R.L., 2014. Correcting midseason crop coefficients
897 for climate. J Irrig Drain Eng. doi:10.1061/(ASCE)IR.1943-4774.0000839.
898
899
900 Hargreaves, G.H., Samani, Z.A., 1985. Reference crop evapotranspiration from temperature.
901 Applied Engineering in Agriculture 1 (2), 96–99, <https://doi.org/10.13031/2013.26773>.
902 USA.

903
904
905
906
907
908
909
910
911
912
913
914
915
916
917
918
919
920
921
922
923
924
925
926
927
928
929
930
931
932
933
934
935
936
937
938
939
940
941
942
943
944
945
946
947
948
949
950

Haylock, M.R., Hofstra, N., Klein Tank, A.M.G., Klok, E.J., Jones, P.D., New, M., 2008. A European daily high resolution gridded data set of surface temperature and precipitation for 1950–2006. *Journal of Geophysical Research* 113, D20119, doi:10.1029/2008JD010201.

Hofstra, N., Haylock, M., New, M., Jones, P.D., 2009. Testing E-OBS European high-resolution gridded data set of daily precipitation and surface temperature. *Journal of geophysical research, atmospheres* 114, Issue D21, doi: 10.1029/2009JD011799.

IPCC, 2007. Fourth IPCC Assessment Report (AR4): Climate Change 2007. Cambridge University Press.

IPCC, 2013. Summary for Policymakers. In: *Climate Change 2013: The Physical Science Basis. Contribution of Working Group I to the Fifth Assessment Report of the Intergovernmental Panel on Climate Change* Stocker, T.F., D. Qin, G.-K. Plattner, M. Tignor, S. K. Allen, J. Boschung, A. Nauels, Y. Xia, V. Bex and P.M. Midgley. Cambridge University Press, Cambridge, United Kingdom and New York, NY, USA.

IPCC, 2014. *Climate Change 2014: Synthesis Report. Contribution of Working Groups I, II and III to the Fifth Assessment Report of the Intergovernmental Panel on Climate Change* [Core Writing Team, R.K. Pachauri and L.A. Meyer (eds.)]. IPCC, Geneva, Switzerland, 151 pp.

IPCC, 2018 A. Summary for Policymakers. In: *Global Warming of 1.5°C. An IPCC Special Report on the impacts of global warming of 1.5°C above pre-industrial levels and related global greenhouse gas emission pathways, in the context of strengthening the global response to the threat of climate change, sustainable development, and efforts to eradicate poverty* [Masson-Delmotte, V., P. Zhai, H.-O. Pörtner, D. Roberts, J. Skea, P.R. Shukla, A. Pirani, W. Moufouma-Okia, C. Péan, R. Pidcock, S. Connors, J.B.R. Matthews, Y. Chen, X. Zhou, M.I. Gomis, E. Lonnoy, T. Maycock, M. Tignor, and T. Waterfield (eds.)]. World Meteorological Organization, Geneva, Switzerland, 32 pp.

IPCC, 2018 B .Hoegh-Guldberg, O., D. Jacob, M. Taylor, M. Bindi, S. Brown, I. Camilloni, A. Diedhiou, R. Djalante, K.L. Ebi, F. Engelbrecht, J. Guiot, Y. Hijikata, S. Mehrotra, A. Payne, S.I. Seneviratne, A. Thomas, R. Warren, and G. Zhou, 2018: Impacts of 1.5°C Global Warming on Natural and Human Systems. In: *Global Warming of 1.5°C. An IPCC Special Report on the impacts of global warming of 1.5°C above pre-industrial levels and related global greenhouse gas emission pathways, in the context of strengthening the global response to the threat of climate change, sustainable development, and efforts to eradicate poverty* [Masson-Delmotte, V., P. Zhai, H.-O. Pörtner, D. Roberts, J. Skea, P.R. Shukla, A. Pirani, W. Moufouma-Okia, C. Péan, R. Pidcock, S. Connors, J.B.R. Matthews, Y. Chen, X. Zhou, M.I. Gomis, E. Lonnoy, T. Maycock, M. Tignor, and T. Waterfield (eds.)]. In Press

- 951 Jones, G.V., Davis, R.E., 2000. Climate Influences on Grapevine Phenology, Grape
952 Composition, and Wine Production and Quality for Bordeaux, France. *American*
953 *Journal of Enology and Viticulture* 51, No. 3.
954
- 955 Kapur, B., Steduto, P., Todorovic, M., 2007. Prediction of climatic change for the next 100
956 years in the Apulia region, Southern Italy. *Italian Journal of Agronomy*, 4, 365-371.
957
- 958 Keuler, K., Radtke, K., Kotlarski, S., Luthi, D., 2016. Regional climate change over Europe in
959 COSMO-CLM: Influence of emission scenario and driving global model,
960 *Meteorologische Zeitschrift*, Vol. 25, No. 2, 121–136.
961
- 962 Kleidon, A., Renner M., 2018. Thermodynamic limits of hydrologic cycling within the Earth
963 system: concepts, estimates and implications. *Hydrology and Earth System Sciences*.
964 17: 2873-2892. DOI: 10.5194/hess-17-2873-2013.
965
- 966 López-Urrea, R., Montoro, A., Manas, F., López-Fuster, P., Fereres, E., 2012.
967 Evapotranspiration and crop coefficients from lysimeter measurements of mature
968 ‘Tempranillo’ wine grapes. *Agricultural Water Management* 112, 13-20.
969
- 970 Lovelli, S., Perniola, M., Di Tommaso, T., Ventrella, D., Moriondo, M., Amato, M., 2010.
971 Effects of rising atmospheric CO₂ on crop evapotranspiration in a Mediterranean area.
972 *Agricultural Water Management*, 97, 1287-1292.
973
- 974 Mancosu, N., 2013. Agricultural water demand assessment using the SIMETAW# model.
975 Ph.D. thesis. University of Sassari.
976
- 977 Mancosu, N., Spano, D., Orang, M., Sarreshteh, S., Snyder, R.L., 2016. SIMETAW#—A
978 Model for Agricultural Water Demand Planning. *Water Resour. Manag.* 30, 541–557,
979 doi:10.1007/s11269-015-1176-7.
980
- 981 Manfreda, S., Fiorentino, M., Iacobellis, V., 2005. DREAM: a distributed model for runoff,
982 evapotranspiration, and antecedent soil moisture simulation. *Adv. Geosci.* 2, 31–39.
983
- 984 Martinez-Cob, A., Tejero-Juste, M., 2004. A wind-based qualitative calibration of the
985 Hargreaves ET₀ estimation equation in semiarid region. *Agricultural Water*
986 *Management* 64 (3), 251–264.
987
- 988 Masia, S., Susnik, J., Marras, S., Mereu, S., Spano, D., Trabucco, A., 2018. Assessment of
989 irrigated agriculture vulnerability under climate change in Southern Italy. *Water (S.I.*
990 *Sustainable Water Management in Agriculture under Global Change)*. 10: 209. DOI:
991 10.3390/w10020209.
992
- 993 Meier, N., Rutishauser, T., Pfister, C., Wanner, H., Luterbacher, J., 2007. Grape harvest dates
994 as a proxy for Swiss April to August temperature reconstructions back to AD 1480.
995 *Geophysical Research Letters* 34, L20705, doi:10.1029/2007GL031381.
996
- 997 Moriondo, M., Bindi, M., Fagarazzi, C., Ferrise, R., Trombi, G., 2011. Framework for high-
998 resolution climate change impact assessment on grapevines at a regional scale. *Reg*
999 *Environ Change* 11:553–567.
1000

- 1001 Nendel, C., 2010. Grapevine bud break prediction for cool winter climates. *International*
1002 *Journal of Biometeorology* 54, 231–241, doi:10.1007/s00484-009-0274-8. Springer.
1003
- 1004 Novello, V., de Palma, L., 2008. Growing grapes under cover. *Actahorticulturae* May 2008,
1005 doi:10.17660/ActaHortic.2008.785.44.
- 1006 OECD, 2017. “Water risk hotspots for agriculture”, OECD, Paris.
1007 [http://www.oecd.org/officialdocuments/publicdisplaydocumentpdf/?cote=COM/TAD/](http://www.oecd.org/officialdocuments/publicdisplaydocumentpdf/?cote=COM/TAD/CA/ENV/EPOC(2016)4/FINAL&docLanguage=En)
1008 [CA/ENV/EPOC\(2016\)4/FINAL&docLanguage=En](http://www.oecd.org/officialdocuments/publicdisplaydocumentpdf/?cote=COM/TAD/CA/ENV/EPOC(2016)4/FINAL&docLanguage=En).
1009
- 1010 Ozdogan, M., 2011. Modeling the impacts of climate change on wheat yields in Northwestern
1011 Turkey. *Agriculture, Ecosystems and Environment* 141, 1–12.
1012
- 1013 Patterson, D.T., Flint, E.P., Beyers, J.L., 1984. Effects of CO₂ Enrichment on Competition
1014 between a C4 Weed and a C3 Crop. *Weed Science* 32, No. 1, 101-105.
1015
- 1016 Picòn-Toro, J., González-Dugo, V., Uriarte, D., Mancha, L.A., Testi, L., 2012. Effects of
1017 canopy size and water stress over the crop coefficient of a “Tempranillo” vineyard in
1018 south-western Spain. *Irrigation Science* 30, 419–432 doi:10.1007/s00271-012-0351-3.
1019
- 1020 Portmann, F.T., Siebert, S., Döll, P., 2010. MIRCA2000 Global monthly irrigated and rainfed
1021 crop areas around the year 2000: A new high resolution data set for agricultural and
1022 hydrological modeling. *Global biogeochemical cycles*, 24, GB1011,
1023 doi:10.1029/2008GB003435.
1024
- 1025 Rockel, B., Will, A., Hense, A., 2008. The regional Climate Model COSMO-CLM (CCLM).
1026 *MeteorologischeZeitschrift* 17 (4), 347-348.
1027
- 1028 Rodriguez-Diaz, J.A., Weatherhead, E.K., Knox, J.W., Camacho, E., 2007. Climate change
1029 impacts on irrigation water requirements in the Guadalquivir river basin in Spain.
1030 *Regional Environment Change* 7, 149–159.
- 1031 Saadi, S., Todorovic, M., Tanasijevic, L., Pereira, L.S., Pizzigalli, C., Lionello, P., 2014.
1032 Climate change and Mediterranean agriculture: Impacts on winter wheat and tomato
1033 crop evapotranspiration, irrigation requirements and yield. *Agricultural Water*
1034 *Management*. Elsevier.
- 1035 Samani, Z., (2000). Estimating solar radiation and evapotranspiration using minimum
1036 climatological data. *Journal of Irrigation and Drainage Engineering*, 126(4), 265-267.
1037
- 1038 Santhi, C., Arnold, J.G., Williams, J.R., Dugas, W.A., Srinivasan, R., Hauck, L.M., 2001.
1039 Validation of the swat model on a large river basin with point and nonpoint sources.
1040 *JAWRA Journal of the American Water Resources Association* 37, 1169–1188.
1041
- 1042 Schulla, J., Jasper, K., 2007. Model Description Wasim-eth. Institute for Atmospheric and
1043 Climate Science, Swiss Federal Institute of Technology, Zurich.
1044
- 1045 Schwab, A.L., Knott, R., Schottdorf, W., 2000. Results from new fungus-tolerant grapevine
1046 varieties for Organic Viticulture. Beitragpräsentiertbei der Konferenz: 6th International
1047 Congress on Organic Viticulture, Basel, Switzerland, 25.08. - 26.08.2000;

1048 Veröffentlicht in Willer, Helga und Meier, Urs, (Hrsg.) Proceedings 6th International
1049 Congress on Organic Viticulture, Seite(n) 225-227. SÖL-Sonderausgabe 77. Stiftung
1050 Ökologie & Landbau, Bad Dürkheim.
1051

1052 Scoccimarro, E., Gualdi, S., Bellucci, A., Sanna, A., Fogli, P.G., Manzini, E., Vichi, M., Oddo,
1053 P., Navarra, A., 2011. Effects of tropical cyclones on ocean heat transport in a high
1054 resolution coupled general circulation model. *Journal of climate* 24 (16), 4368–4384.
1055

1056 SDSN, 2019. Cresti S. SDGs: The Mediterranean is Still Lagging Behind Sustainable
1057 Development Solutions Network.
1058

1059 Siad, Si M., Iacobellis, V., Zdruli, P., Gioia, A., Stavi, I., Hoogenboom, G., 2019. A review of
1060 coupled hydrologic and crop growth models, *Agricultural Water Management*,
1061 10.1016/j.agwat.2019.105746, 224, (105746).

1062 Snyder, R.L., Geng, S., Orang, M., Sarreshteh, S., 2012. Calculation and Simulation of
1063 Evapotranspiration of Applied Water. *Journal of Integrative Agriculture* 11(3), 489–
1064 501, [https://doi.org/10.1016/S2095-3119\(12\)60035-5](https://doi.org/10.1016/S2095-3119(12)60035-5).
1065

1066 de Sousa Lima, J., Antonino, A., Souza, E., Hammecker, C., Montenegro, S., Lira, C., 2013.
1067 Calibration of Hargreaves-Samani equation for estimating reference evapotranspiration
1068 in the sub-humid region of Brazil. *Journal of Water Resource and Protection* 5, 12A.
1069

1070 Steduto, P., Hsiao, T.C., Raes, D., Fereres, E., 2009. AquaCrop-The FAO Crop Model to
1071 Simulate Yield Response to Water: I. Concepts and Underlying Principles. *Agronomy*
1072 *Journal*, 101(3): 426-437. Crop Yield Response to Water. FAO Irrigation and Drainage
1073 Paper 66. By P. Steduto, T. C. Hsiao, E. Fereres and D. Raes. Rome, Italy: Food and
1074 Agriculture Organization of the United Nations, 2012). pp. 500. ISBN 978-92-5-
1075 107274-5. <http://www.fao.org/docrep/016/i2800e/i2800e00.htm>.
1076

1077 Stockle, C.O., Donatelli, M., Nelson, R., 2003. CropSyst, a cropping systems simulation
1078 model. *European Journal of Agronomy*, 18 (3): 289-307.
1079

1080 Supit, I., van Diepen, C.A., Boogaard, H.L., Ludwig, F., Baruth, B., 2010. Trend analysis of
1081 the water requirements, consumption and deficit of field crops in Europe. *Agric. Forest*
1082 *Meteorol.* 150, 77–88.
1083

1084 Tanasijevic, L., Todorovic, M., Pereira, L.S., Pizzigalli, C., Lionello, P., 2014. Impacts of
1085 climate change on olive crop evapotranspiration and irrigation requirements in the
1086 Mediterranean region. *Agricultural Water Management* 144, 54–68. Elsevier.
1087

1088 Taylor, K.E., Stouffer, R.J., Meehl, G.A., 2012. An overview of CMIP5 and the experiment
1089 design. *Bulletin of the American Meteorological Society* 93 (4), 485-498.
1090

1091 Temesgen, B., Allen, R.G., Jensen, D.T., 1999. Adjusting temperature parameters to reflect
1092 well-water conditions. *Journal of Irrigation and Drainage Engineering* 125 (1), 26–33.
1093

1094 Templ, B., Koch, E., Bolmgren, K., Ungersböck, M., Paul, A., Scheifinger, H., et al.
1095 2018. Pan European Phenological database (PEP725): a single point of access for

1096 European data. *Int. J. Biometeorology*. doi: 10.1007/s00484-018-1512-8
1097 <http://www.pep725.eu/>.
1098
1099 Tomasi, D., Jones, G.V., Giust, M., Lovat, L., Gaiotti, F., 2011. Grapevine Phenology and
1100 Climate Change: Relationships and Trends in the Veneto Region of Italy for 1964-2009.
1101 *American Journal of Enology and Viticulture (AJEV)*, doi: 10.5344/ajev.2011.10108.
1102
1103 Tubiello, F.N., Donatelli, M., Rosenzweig, C., Stockle, C.O., 2000. Effects of climate change
1104 and elevated CO₂ on cropping systems: Model predictions at two Italian locations.
1105 *European Journal of Agronomy* 13, 179–189.
1106
1107 Twine, T.E., Kustas, W.P., Norman, J.M., Cook, D.R., Houser, P.R., Meyer, T.P., Pruege, J.H.,
1108 Starks, P.J., Wesely, M.L., 2000. Correcting eddy-covariance flux underestimates over
1109 a grassland. *Agricultural and Forest Meteorology* 103, 279-300.
1110
1111 Valdés-Gómez, H., Celette, F., de Cortázar-Atauri, I.G., Jara-Rojas, F., Ortega-Farías, S., Gary,
1112 C., 2009. Modelling Soil Water Content And Grapevine Growth And Development
1113 With The Stics Crop-Soil Model Under Two Different Water Management Strategies.
1114 *Journal International des Sciences de la Vignee et du Vin* 43, No.1, 13-28.

1115 Valizadeh, J., Ziaei, S.M., Mazloumzadeh, S.M., 2014. Assessing climate change impacts on
1116 wheat production (a case study). *Journal of the Saudi Society of Agricultural Sciences*
1117 13, 107-115.
1118
1119 van Diepen, C.A., Wolf, J., van Keulen, H., Rappoldt, C., 1989. WOFOST: a simulation
1120 model of crop production. *Soil Use Manag.* 5, 16–24.
1121
1122 Wieder, W.R., Boehnert, J., Bonan, G.B., Langseth, M., 2014. RegridDED Harmonized
1123 World Soil Database v1.2. Data set. Available on-line [<http://daac.ornl.gov>] from
1124 Oak Ridge National Laboratory Distributed Active Archive Center, Oak Ridge,
1125 Tennessee, USA.,
1126
1127 Williams, J.R., 1990. The erosion-productivity impact calculator (EPIC) model: a case history.
1128 *Philosophical Transactions: Biological Sciences*: 421-428.
1129
1130 Wilson, K., Goldstein, A, Falge, E., Aubinet, M., Baldocchi, D., Berbigier, P., Bernhofer, C.,
1131 Ceulemans, R., Dolman, H., Field, C., Grelle, A., Ibrom, A., Law, B.E., Kowalski, A.,
1132 Meyers, T., Moncrieff, J., Monson, R., Oechel, W., Tenhunen, J., Valentini, R., Verma,
1133 S., 2002. Energy balance closure at FLUXNET sites. *Agricultural and Forest*
1134 *Meteorology* 113, 223-243.

1135 Yano, T., Aydin, M., Haraguchi, T., 2007. Impact of climate change on irrigation demand and
1136 crop growth in a Mediterranean environment of Turkey. *Sensors* 7, 2297-2315.
1137
1138 You, L., Wood-Sichra, U., Fritz, S., Guo, Z., See, L., Koo, J., 2014. Spatial Production
1139 Allocation Model (SPAM) 2005 v2.0. March 7, 2017. Available from
1140 <http://mapspam.info>.
1141
1142
1143

1144 **Websites**

1145
 1146 Climate-ADAPT, 2016. [https://climate-adapt.eea.europa.eu/metadata/adaptation-](https://climate-adapt.eea.europa.eu/metadata/adaptation-options/improvement-of-irrigation-efficiency)
 1147 [options/improvement-of-irrigation-efficiency](https://climate-adapt.eea.europa.eu/metadata/adaptation-options/improvement-of-irrigation-efficiency).
 1148
 1149 CORDEX. <https://www.hzg.de/ms/clm-community/076427/index.php.en> Last access 2019.
 1150
 1151 FAO, 2016. http://www.fao.org/nr/water/aquastat/tables/WorldData-Withdrawal_eng.pdf.
 1152
 1153 FAOSTAT. <http://www.fao.org/faostat/en/#data/QC>. Last access 2016.
 1154
 1155 FLUXNET: <https://fluxnet.ornl.gov/>. Last access 2016.
 1156
 1157 World Bank, 2017. <https://www.worldbank.org/en/topic/water-in-agriculture#2>.
 1158

1159

1160 **Appendix 1**

1161

ID	ZONE NAME	Grape - Bud break literature
5	Algeria	Same as Morocco
15	Austria	Templ et al., 2018
26	Bosnia and Herzegovina	Templ et al., 2018
35	Bulgaria	Same as Romania
66	Egypt	Same as Morocco
74	Czechia	Same as Slovakia
83	France	Jones and Davis 2000; Andreini et al., 2009; Valdez-Gomez et al., 2009; Nendel, 2010
93	Germany	Templ et al., 2018; Nendel, 2010; Schwab et al., 2000
97	Greece	Anderson et al., 2014
106	Croatia	Templ et al., 2018
107	Hungary	Same as Slovakia
116	Italy	Cortesi et al., 1997; Novello and Palma 2008; Tomasi et al. 2011; Mancosu, 2013
140	Slovakia	Templ et al., 2018; Nendel 2010
153	Macedonia	Same as Greece
156	Morocco	Ezzhaouani et al., 2007
189	Portugal	Same as Spain
196	Romania	Same as Greece and Slovakia
201	Saudi	Same as Morocco
208	Slovenia	Same as Croatia
213	Spain	Camps and Ramos 2012; Lopez - Urrea et al. 2012; Picon - Toro et al., 2012
214	Serbia	Same as Bosnia
220	Syrian	Same as Greece
221	Switzerland	Same as Austria
231	Tunisia	Same as Morocco
232	Turkey	Same as Greece

1162

1163

ID	ZONE NAME	Grape - Harvest literature
5	Algeria	Same as Morocco
15	Austria	Templ et al., 2018
26	Bosnia and Herzegovina	Templ et al., 2018
35	Bulgaria	Same as Romania
66	Egypt	Same as Morocco
74	Czechia	Same as Slovakia
83	France	Jones and Davis, 2000; Valdez-Gomez et al., 2009
87	Georgia	Same as Greece
93	Germany	Templ et al., 2018; Schwab et al., 2000; Christoph et al., 2003
97	Greece	Anderson et al., 2014
106	Croatia	Same as Italy
107	Hungary	Same as Austria
116	Italy	Tomasi et al., 2011; Mancosu, 2013
140	Slovakia	Same as Austria
153	Macedonia	Same as Greece

156	Morocco	Ezzhaouani et al., 2007
189	Portugal	Same as Spain
196	Romania	Same as Greece and Slovakia
201	Saudi	Same as Morocco
208	Slovenia	Same as Italy
213	Spain	Camps and Ramos 2012; Lopez - Urrea et al. 2012; Picon - Toro et al., 2012
214	Serbia	Same as Bosnia
220	Syrian	Same as Greece
221	Switzerland	Templ et al., 2018; Meier et al., 2007
231	Tunisia	Same as Morocco
232	Turkey	Same as Greece

1164

1165

A Modeling Tool to Assess the Impact of Climate Change on Crop Water Requirement at Local and Regional Scale

Figures:

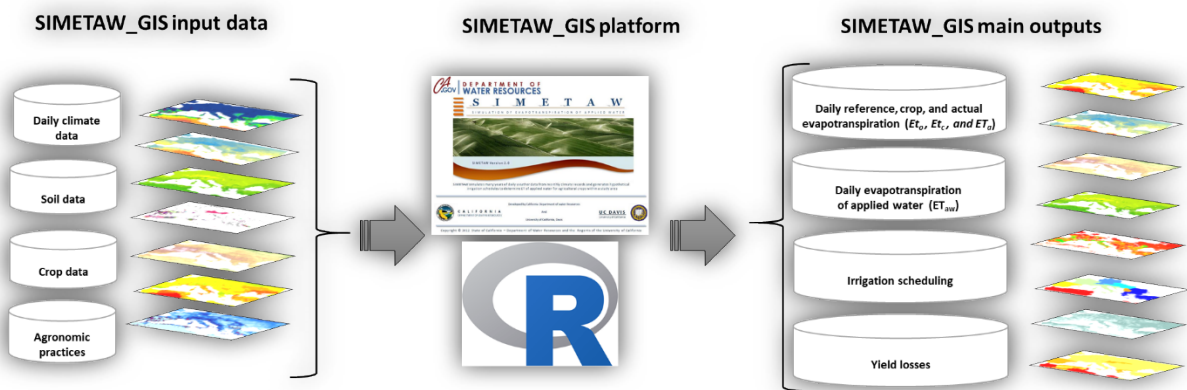


Fig. 1. Scheme of SIMETAW_GIS platform.

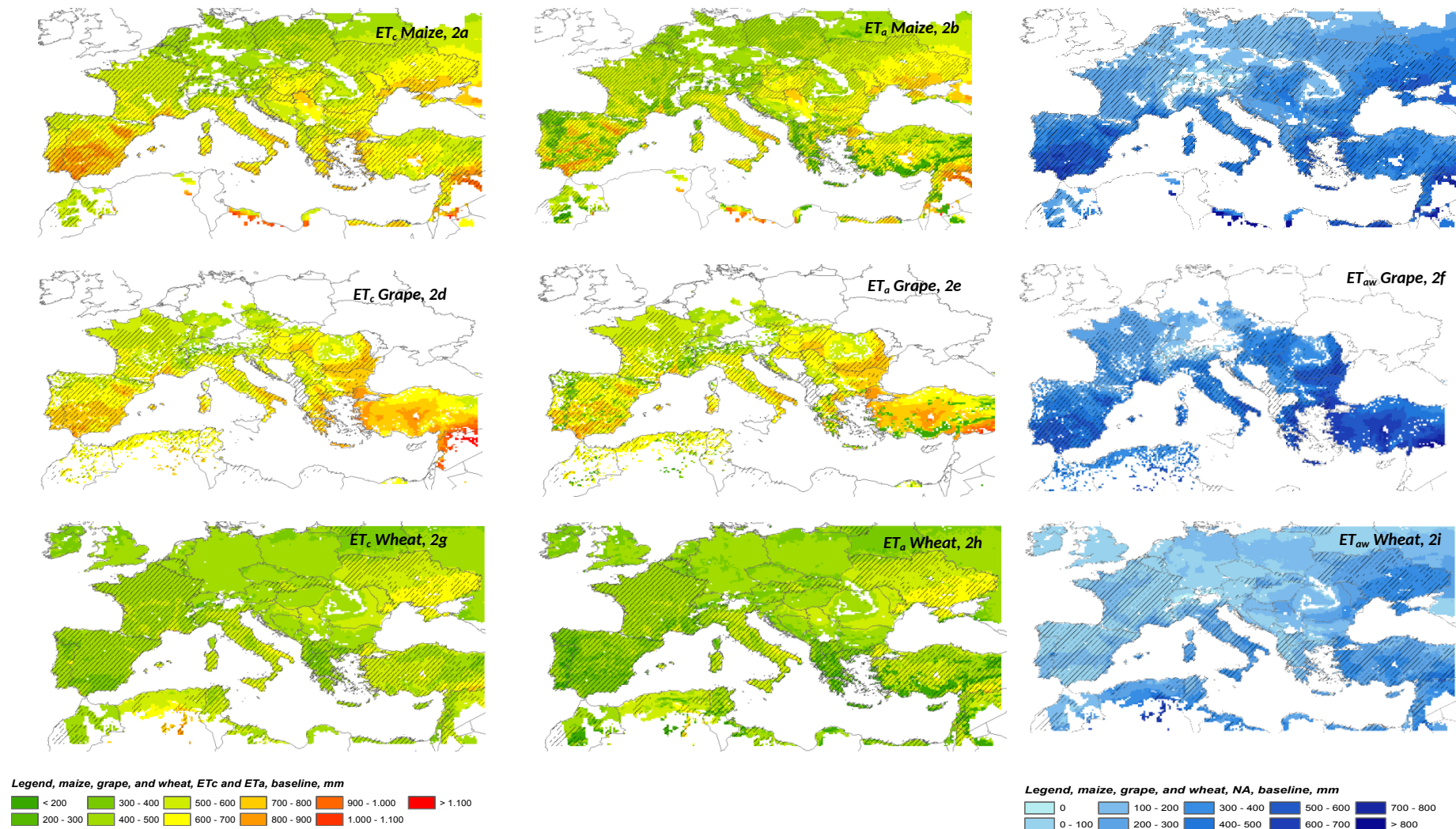


Fig. 2. Regional mean of ET_c (2a, 2d, 2g), ET_a (2b, 2e, and 2h) and ET_{aw} (2c, 2f, and 2i) for maize, grape and wheat during 1976-2005 considering potential crop distribution widespread in the entire domain. The effective crop irrigated areas are distinguished using solid diagonals lines.

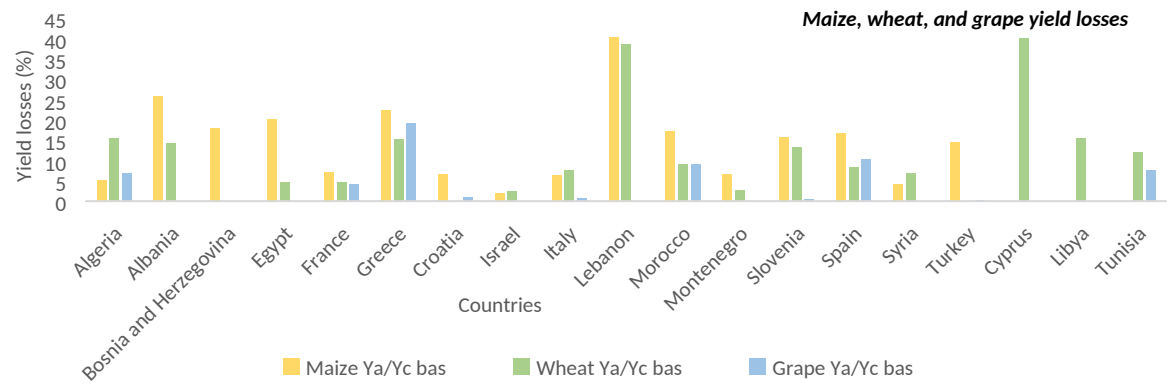


Fig. 3. Regional mean yield responses to water deficit (Y_d/Y_c) for maize, grape and wheat during 1976-2005.

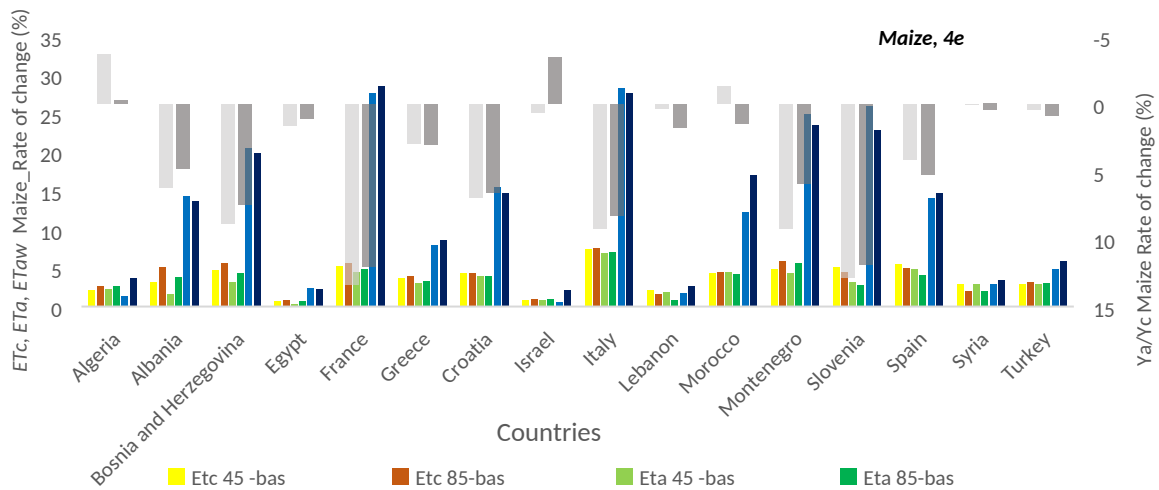
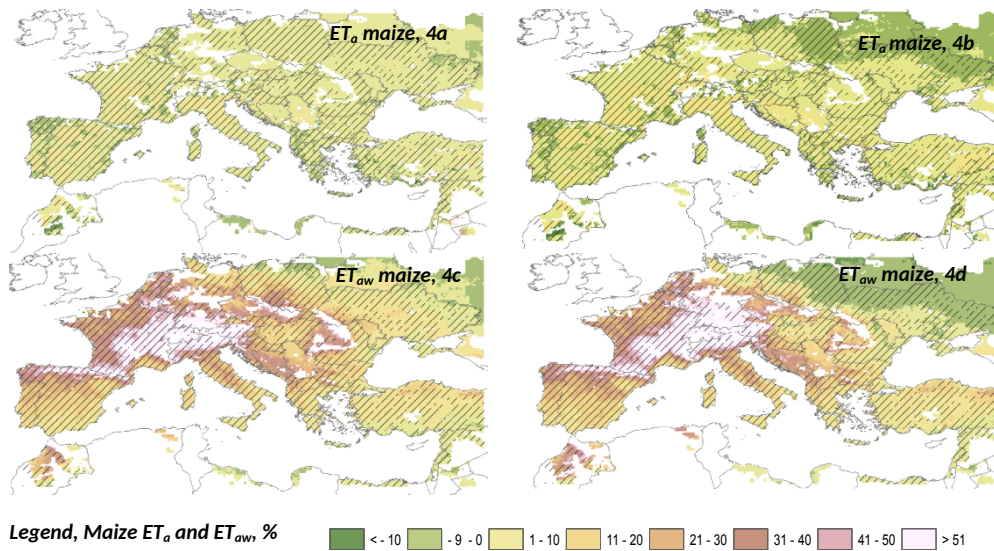


Fig. 4. Rate of change of ET_a (4a. ET_a 45-bas, 4b. ET_a 85-bas) and ET_{aw} (4c. ET_{aw} 45-bas, 4d. ET_{aw} 85-bas) values weighted for the irrigated maize distribution between future climate condition (2036-2065) under both RCP 4.5 and 8.5 scenarios, and the baseline (1976-2005) for the entire domain with a focus on the Mediterranean countries (Fig. 4e). Rate of changes of maize ET_c (ET_c 45-bas, ET_c 85-bas) and yield losses (Y_a/Y_c 45-bas, Y_a/Y_c 85-bas) between future and baseline period in the Mediterranean countries are shown in figure 4e.

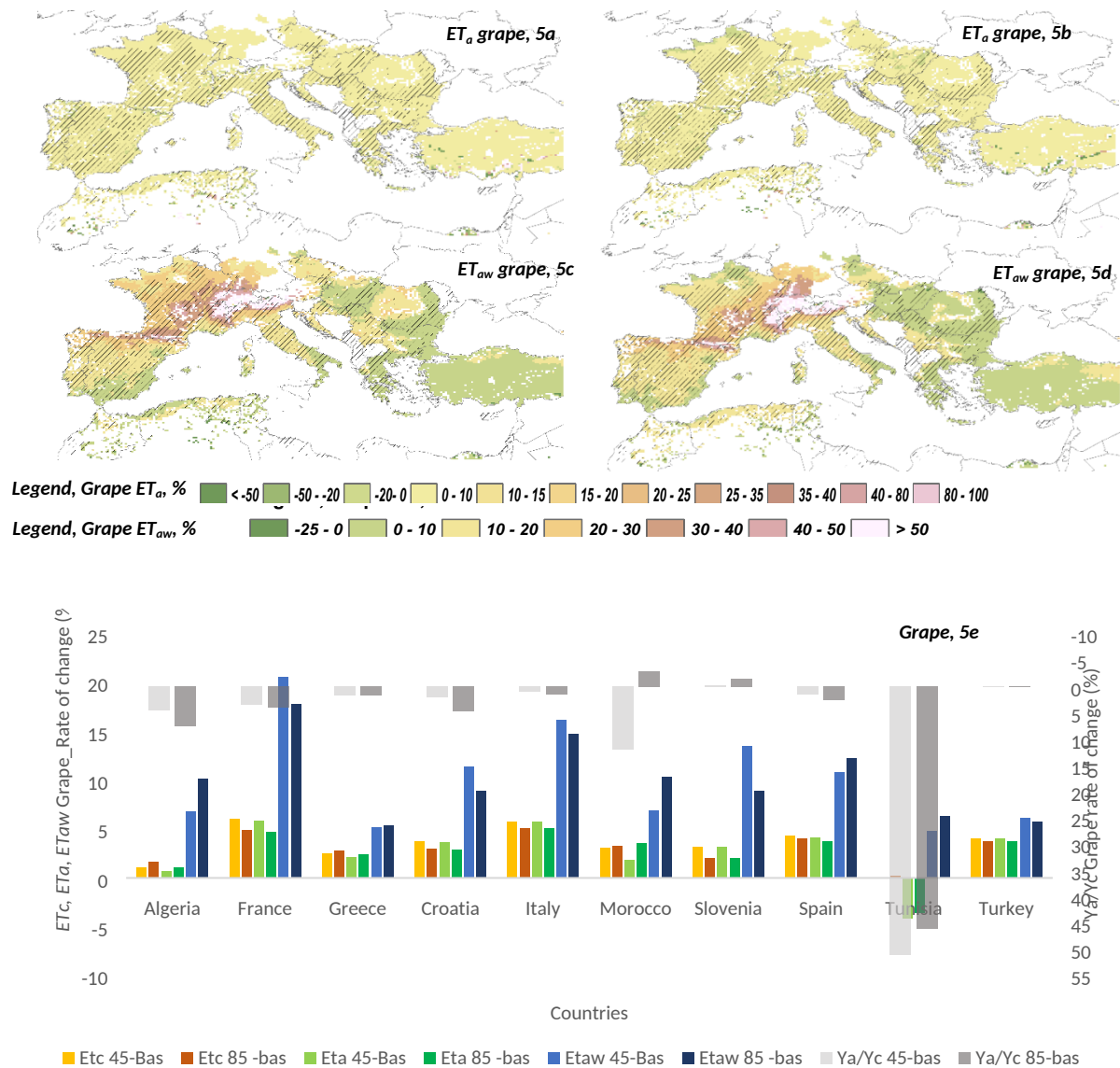
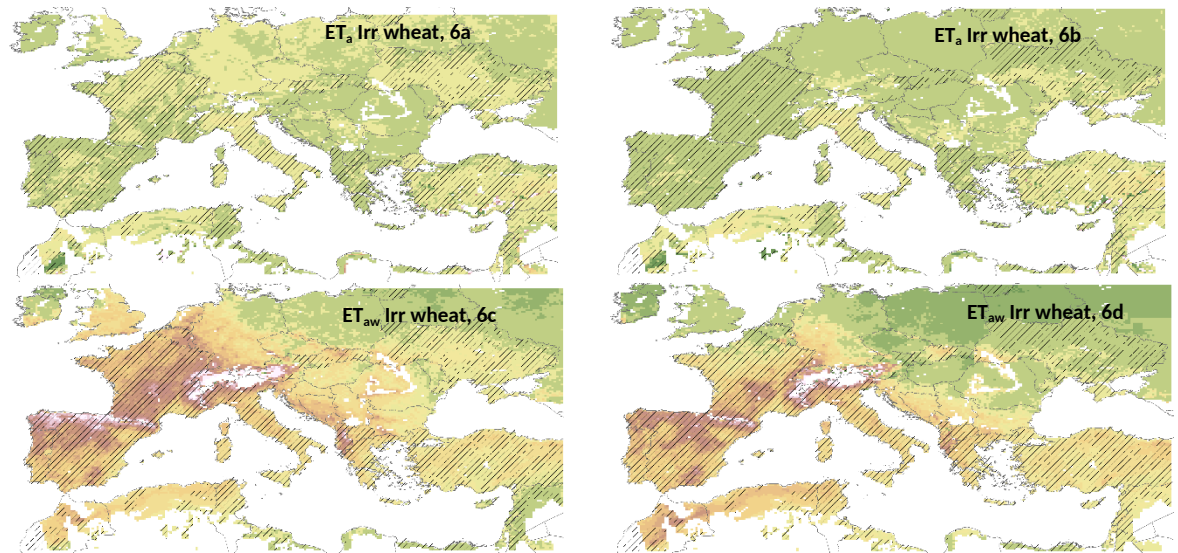


Fig. 5. Rate of change of ET_a (5a. ET_a 45-bas, 5b. ET_a 85-bas) and ET_{aw} (5c. ET_{aw} 45-bas, 5d. ET_{aw} 85-bas) values weighted for the irrigated grape distribution between future climate condition (2036-2065) under both RCP 4.5 and 8.5 scenarios, and the baseline (1976-2005) for the entire domain with a focus on the Mediterranean countries (Fig. 5e). Rate of changes of maize ET_c (ET_c 45-bas, ET_c 85-bas) and yield losses (Y_d/Y_c 45-bas, Y_d/Y_c 85-bas) between future and baseline period in the Mediterranean countries are shown in figure 5e.



Legend, Irr Wheat ET_a and ET_{aw} %

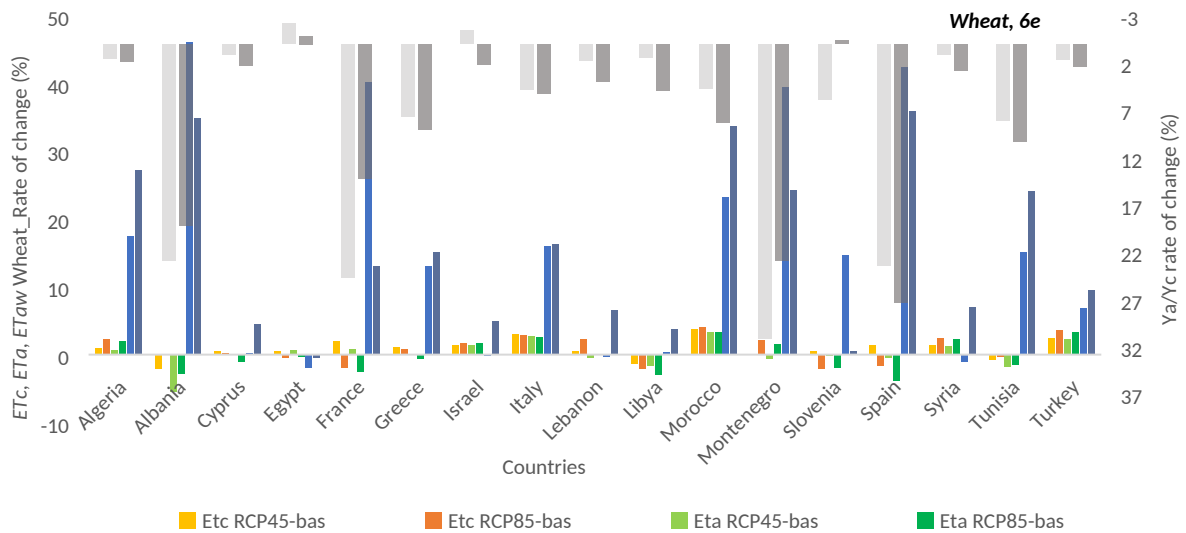


Fig. 6. Rate of change of ET_a (6a. RCP45-bas, 6b. RCP85-bas) and ET_{aw} (6c. RCP45-bas, 6d. RCP85-bas) values weighted for the irrigated wheat distribution between future climate condition (2036-2065) under both RCP 4.5 and 8.5 scenarios, and the baseline (1976-2005) with a focus on the Mediterranean countries (Fig. 6e). Rate of changes of wheat yield losses between future and baseline period are shown in figure 6e.

A Modeling Tool to Assess the Impact of Climate Change on Crop Water Requirement at Local and Regional Scale

Tables:

Tab.1. Crop characteristics and experimental sites selected through the FLUXNET network.

<i>Code</i>	<i>SITE</i>	<i>Country</i>	<i>Lat</i>	<i>Lon</i>	<i>Elevation (m.a.s.l.)</i>	<i>Crop</i>	<i>Sowing-Harvest date</i>
IT-Neg	Negrisia	Italy	45.75	12.45	11	Wine Grape	01.04.2007/15.10.2007
IT-Neg	Negrisia	Italy	45.75	12.45	11	Wine Grape	01.04.2008/27.10.2008
IT-VdA	Valle dell'Adige	Italy	46.20	11.11	207	Wine Grape	15.04.2009/05.09.2009
IT-BCi	Borgo Cioffi	Italy	40.52	14.96	13	Maize	17.05.2005/24.08.2005
IT-BCi	Borgo Cioffi	Italy	40.52	14.96	13	Maize	27.04.2006/22.08.2006
IT-BCi	Borgo Cioffi	Italy	40.52	14.96	13	Maize	09.05.2007/24.08.2007
IT-BCi	Borgo Cioffi	Italy	40.52	14.96	13	Maize	12.06.2009/08.09.2009
DE-Kli	Klingenberg	Germany	50.89	13.52	468	Wheat	25.09.2005/06.09.2006
DE-Kli	Klingenberg	Germany	50.89	13.52	469	Maize	23.04.2007/2.10.2007
DE-Geb	Gebesee	Germany	51.10	10.91	157	Wheat	09.11.2006/07.08.2007
FR-Lam	Lamasquere	France	43.50	1.24	182	Wheat	18.10.2006/15.07.2007
FR-Lam	Lamasquere	France	43.50	1.24	182	maize	01.05.2006/31.08.2006
FR-Gri	Grignon	France	48.84	1.95	117	wheat	28.10.2005/15.07.2006
FR-Gri	Grignon	France	48.84	1.95	117	maize	09.5.2005/28.09.2005
CH-Oe2	Oensingen	Switzerland	47.29	7.73	450	wheat	19.10.2006/16.07.2007
BE-Lon	Lonzee	Belgium	50.55	4.75	165	wheat	14.10.2004/03.8.2005
BE-Lon	Lonzee	Belgium	50.55	4.75	165	wheat	13.10.2006/05.08.2007
NL-Dij	Dijgraaf	The Netherlands	51.99	5.65	9	maize	08.05.2007/27.09.2007

Tab. 2. SIMETA_R performance shown through the comparison of observed and modelled ET_a in ten experimental sites. Measured data quality are shown through statistical indices, the energy balance closure (EBC) and the correlation between LE measured and LE residual (LE vs LE').

Code	YEAR	Crop	Observed ET _a vs Modelled ET _a					EBC			LE vs LE'
			r	RMSE mm	IA %	MBE mm	MBA mm	R ² %	Y = aX + b	Gaps %	r
FR-Gri	2005	Corn	0.81	0.75	89	0.04	0.63	91	Y = 0.7583X	19	0.89
FR-Gri	2005-2006	Wheat	0.85	0.61	91	0.12	0.45	87	Y = 0.6748X	16	0.87
DE-Geb	2006-2007	Wheat	0.75	1.14	78	0.69	0.78	77	Y = 0.7335X	15	0.85
DE-Kli	2007	Corn	0.84	1.39	67	1.23	1.24	56	Y = 0.4694X	32	0.61
DE-Kli	2005-2006	Wheat	0.88	0.82	88	0.57	0.65	67	Y = 0.8379X	33	0.62
CH-Oe2	2006-2007	Wheat	0.92	0.75	94	-0.44	0.58	68	Y = 0.8037X	34	0.82
NL-Dij	2007	Corn	0.71	0.68	82	-0.14	0.54	73	Y = 0.7905X	15	0.87
FR-Lam	2006-2007	Wheat	0.82	0.72	90	-0.23	0.55	83	Y = 0.7254X	41	0.83
FR-Lam	2006	Corn	0.61	1.22	76	0.43	0.92	90	Y = 0.7838X	42	0.91
BE-Lon	2006-2007	Wheat	0.78	0.91	82	0.57	0.72	82	Y = 0.8487X	20	0.84
BE-Lon	2004-2005	Wheat	0.89	0.89	90	0.14	0.65	82	Y = 0.8454X	23	0.85
IT-Bci	2005	Corn	0.64	1.21	73	0.62	0.92	92	Y = 0.7794X	26	0.92
IT-Bci	2006	Corn	0.62	1.29	69	0.73	0.97	86	Y = 0.7894X	39	0.82
IT-Bci	2007	Corn	0.63	1.48	68	0.93	1.12	94	Y = 0.778X	37	0.95
IT-Bci	2009	Corn	0.63	1.32	75	0.51	1.03	91	Y = 0.7405X	50	0.94
IT-VdA	2009	Wine Grape	0.82	0.68	90	0.06	0.5	77	Y = 0.6866X	23	0.93
IT-Neg	2007	Wine Grape	0.83	1.91	77	1.3	1.6	na*	na*	na*	na*
IT-Neg	2008	Wine Grape	0.58	2.45	67	1.31	1.88	na*	na*	na*	na*

Tab. 3. Assessment of modelled ET_o computed using Hargreaves (with E-OBS and EI gridded data) and Penman Monteith (EI gridded data) equation against site observations (FLUXNET sites). Values are expressed as a mean of the values estimated in each site and for each available growing season.

HS_EOBS vs HS_site	HS_EI vs HS_site	PM_EI vs PM_site
<i>RMSE (mm)</i>		
1.74	1.85	1.01
<i>MBE (mm)</i>		
0.86	0.89	-0.03
<i>MAE (mm)</i>		
1.49	1.59	0.79
<i>IA (%)</i>		
59	59	81

Tab. 4. Precipitation values in the baseline period (pcp bas, mm) and climate anomalies (%) in the Mediterranean Countries for RCP 4.5 and 8.5 scenarios

	Algeria	Albania	Bosnia and Herzegovina	Cyprus	Croatia	Egypt	France	Greece	Israel	Italy
pcp bas	185	1095	1026	165	895	38	882	521	134	834
pcp45-bas	-15.75	-9.56	-7.45	-0.62	-4.66	0	-2.97	-18.35	5.65	-7.52
pcp85-bas	-26.08	-6.39	-5.65	-12.37	1.08	5.29	0.12	-16.21	-0.96	-7.54
	Lebanon	Libya	Morocco	Montenegro	Slovenia	Spain	Syria	Tunisia	Turkey	
pcp bas	397	76	352	1441	1084	711	146	163	479	
pcp45-bas	-3.08	-13.21	-19.01	-9.53	-2.61	-10.48	4.3	-15.9	-6.35	
pcp85-bas	-14.33	-22.79	-27.49	-4.81	5.5	-6	-6.43	-28.7	-8.52	